

# Distances Between Top-Truncated Elections of Different Sizes

Piotr Faliszewski<sup>1</sup>, Jitka Mertlová<sup>2</sup>, Pierre Nunn<sup>3</sup>, Stanisław Szufa<sup>4</sup>, Tomasz Wąs<sup>5</sup>

<sup>1</sup>AGH University

<sup>2</sup>Czech Technical University in Prague

<sup>3</sup>Université de Rennes

<sup>4</sup>CNRS, LAMSADE, Université Paris Dauphine-PSL

<sup>5</sup>University of Oxford

faliszew@agh.edu.pl, mertlova.jita@gmail.com, pierre.nunn@ens-rennes.fr, s.szufa@gmail.com, tomasz.was@cs.ox.ac.uk

## Abstract

The map of elections framework is a methodology for visualizing and analyzing election datasets. So far, the framework was restricted to elections that have equal numbers of candidates, equal numbers of voters, and where all the (ordinal) votes rank all the candidates. We extend it to the case of elections of different sizes, where the votes can be top-truncated. We use our results to present a visualization of a large fragment of the Preflib database.

**Code** — <https://github.com/Project-PRAGMA/Map-Different-Sizes-AAAI-2025>

## 1 Introduction

The map of elections framework is a methodology for analyzing and visualizing sets of elections, introduced by Szufa et al. (2020) and Boehmer et al. (2021). The basic idea is to depict (ordinal) elections as points on a plane, so that the closer two given points are, the more similar are their corresponding elections (see Figures 1a and 1b for examples, and Section 2 for definitions). To measure this similarity, one can either use the accurate but computationally challenging isomorphic swap distance (Faliszewski et al. 2019), or the less precise but efficiently computable positionwise distance (Szufa et al. 2020), or whatever other distance that is invariant to renaming the candidates and voters. Indeed, the elections may be unrelated to each other and we only care about their structural similarities. Unfortunately, the distances used so far are restricted to elections with the same numbers of candidates and voters, and require the votes to be complete, i.e., to rank all the candidates. We aim to rectify these two issues.

The original motivation behind the map framework was to better understand relations between various statistical cultures (i.e., models of generating random elections) and to present experimental results in a nonaggregate way (Szufa et al. 2020). For this, the restriction to particular election sizes and complete votes is natural, as we have full control over the data. However, maps are also useful for studying real-life elections. For example, we can get better insight into the nature of real-life elections by analyzing their positions on the map (Boehmer et al. 2021; Boehmer and

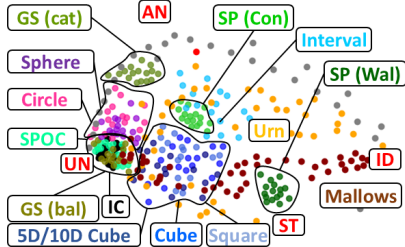
Schaar 2023), or check which statistical cultures yield similar elections (Boehmer et al. 2021, 2022a). Yet, real-life data poses some issues, as seen in the next two datasets from Preflib (Mattei and Walsh 2013):

**Irish General Elections.** Preflib includes the ordinal votes cast in several constituencies in Ireland during the 2002 general election. Naturally, each of them had a different number of candidates (between 9 and 14) and a different number of voters (between around 30 000 and 64 000), most of whom ranked some top candidates only.

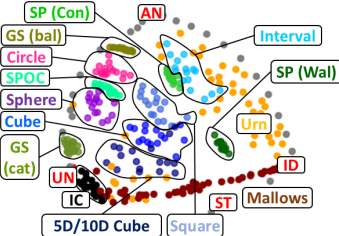
**Formula 1.** Here, each election is a Formula 1 season, where each vote is a race ranking the drivers (i.e., the candidates) in the order in which they finished. There are around 20 races and 20 drivers in each season, but these numbers vary, and not all drivers complete each race.

So far, to put such elections on a map, one had to fill in the missing parts of the preference orders, restrict the number of candidates to some common value (e.g., by deleting the worst-performing ones), and sample a fixed-size set of votes. We propose distances that can deal with different-sized/top-truncated elections natively, without preprocessing.

Ideally, we would like to extend the isomorphic swap and positionwise distances so that different-sized elections with “obviously identical” structure would be at distance zero. Unfortunately, this turns out to be impossible even for a rather minimal definition of an “obviously identical” structure (even without thinking of top-truncated votes). However, we do find two intuitively appealing distances that fulfill some of our requirements: One is an extension of the positionwise distance and one, which we call DAP, is based on analyzing diversity, agreement, and polarization within votes. In the spirit of our desiderata, DAP turns out to be strongly correlated with the isomorphic swap distance and, so, can serve as its replacement. We first describe our distances and then analyze their properties, both theoretically and experimentally. In the experiments, we largely focus on synthetic elections, as such data is easier to control, but our main motivation is to visualize real-life data. Hence, in Section 5 we form a map of a large fragment of Preflib, a database of real-life elections (see Figure 4). The overarching goal of the paper is to explain how we obtained this map, why the choices made on the way are justified, and what we can learn from it.



(a) Positionwise Distance.



(b) Swap Distance.

Figure 1: Maps of elections created using the (a) isomorphic swap and (b) positionwise distances. Each point corresponds to an election; the color represents the statistical culture it comes from: ID, UN, and AN refer to identity, uniformity, and antagonism elections; IC, Mallows, and urn mean impartial culture, the normalized Mallows model, and the Pólya-Eggenberger urn model, respectively; Interval, Square, Cube, 5D/10D Cube, Circle, and Sphere refer to Euclidean models; SP stands for single-peaked (in the Conitzer or Walsh models), SPOC for single-peaked on a circle, and GS for group-separable (caterpillar or balanced).

## 2 Preliminaries

For a positive integer  $k$ , we let  $[k] = \{1, \dots, k\}$ , and we write  $\mathbb{R}_+$  to denote the set of nonnegative real numbers. For two equal-sized sets  $A$  and  $B$ ,  $\Pi(A, B)$  is the set of bijections between  $A$  and  $B$ .

**Elections.** An *election* is a pair  $E = (C, V)$ , where  $C$  is a set of  $m$  *candidates* and  $V$  is a collection of  $n$  *votes*, i.e., weak orders over  $C$ ; we will also sometimes refer to members of  $V$  as *voters* (i.e., the agents who cast the respective votes). By a *size* of an election, we mean the pair  $(m, n)$ . For two candidates  $a, b \in C$  and voter  $v \in V$ , we write  $a \succ_v b$  if  $v$  strictly prefers  $a$  over  $b$  and  $a \sim_v b$  if  $v$  is indifferent between them. We write  $a \succeq_v b$  if  $a \succ_v b$  or  $a \sim_v b$ . By  $N_E(a \succ b)$  we mean the number of voters in election  $E$  that strictly prefer  $a$  to  $b$ , and by  $N_E(a \sim b)$  we mean the number of those indifferent between these candidates.

Consider vote  $v$  over candidate set  $C$ . We say that  $v$  is *complete* if it is a strict linear order over  $C$ , and that it is *top-truncated* if  $C$  can be partitioned into sets  $C_v^\uparrow$  and  $C_v^\downarrow$ , so that  $v$  is a strict linear order over  $C_v^\uparrow$  and for every  $c \in C_v^\uparrow$  and  $a, b \in C_v^\downarrow$  we have  $c \succ_v a \sim_v b$ .  $C_v^\uparrow$  is the top part of  $v$  and  $C_v^\downarrow$  is its truncated part (so a complete vote is top-truncated with empty truncated part.) An election is complete (top-truncated) if all its votes are complete (top-truncated).

Top-truncated elections are quite common in real-life election data (see e.g., *Preflib* database (Mattei and Walsh 2013)) and have been extensively studied in terms of their prevalence (Kilgour, Grégoire, and Foley 2020), efficiency (Borodin et al. 2022), effect on voting rules (Tomlinson, Ugander, and Kleinberg 2023), or a possibility of manipulation (Baumeister et al. 2012).

**Special Elections.** Following Boehmer et al. (2021), we consider the following families of characteristic (complete) elections (we consider  $m$  candidates and  $n$  voters): (i) In an *identity election* ( $ID_{m,n}$ ) all  $n$  votes are identical; (ii) an *antagonism election* ( $AN_{m,n}$ ) is a concatenation of two identity ones, where the voters in one have opposite preference orders to those in the other; and (iii) in a *uniformity election* ( $UN_{m,n}$ ) all possible votes appear equal number of times. The number of voters must be even in an antagonism elec-

tion and must be a multiple of  $m!$  in a uniformity one. We drop the number of voters from notation when it is irrelevant.

**Distances.** A *pseudodistance* over a set  $U$  is a function  $d: U \times U \rightarrow \mathbb{R}_+$  such that for each  $a, b, c \in U$  we have (1)  $d(a, a) = 0$ , (2)  $d(a, b) = d(b, a)$ , and (3)  $d(a, b) + d(b, c) \geq d(a, c)$ . We often drop “pseudo” prefix.

**(Isomorphic) Swap Distance.** Given two votes,  $u, v$ , over the same candidate set, we define their swap distance as  $\text{swap}(u, v) = \frac{1}{2} \sum_{a, b \in C} ([a \succ_u b \wedge b \succeq_v a] + [a \succeq_u b \wedge b \succ_v a])$ , where the expressions in square brackets evaluate to 1 when they are true and to 0 otherwise. That is, we add 1 for each pair of candidates for which both voters have a strict, opposite preference, and we add  $1/2$  for each pair of candidates for which exactly one of the voters is indifferent.

For a pair of equal-sized/complete elections  $E = (C, V)$  and  $F = (D, U)$ , such that  $|C| = |D| = m$ ,  $V = \{v_1, \dots, v_n\}$  and  $U = \{u_1, \dots, u_n\}$ , their *(isomorphic) swap distance* is the sum of the swap distances between the votes, under optimal matchings of the candidates and voters. Formally,  $d_{\text{swap}}(E, F)$  is equal to:

$$\min_{\pi \in \Pi([n], [n])} \sum_{\sigma \in \Pi(C, D)} \text{swap}(\sigma(v_i), u_{\pi(i)}) / (\frac{1}{4}n(m^2 - m)),$$

where  $\sigma(v_i)$  means vote  $v_i$  with each candidate  $c \in C$  replaced with  $\sigma(c) \in D$ . By definition,  $d_{\text{swap}}$  is invariant to renaming the candidates and reordering the voters, and its value is zero if and only if the given elections are isomorphic (i.e., are identical up to renaming the candidates and reordering the voters). This distance was introduced by Faliszewski et al. (2019). Dividing by  $\frac{1}{4}n(m^2 - m)$  ensures normalization of the largest distance to exactly 1 (for the case where  $n$  is even (Boehmer et al. 2022b)).

**Wasserstein Distance.** Given a vector  $\vec{a} = (a_1, \dots, a_m) \in \mathbb{R}_+^m$ , we identify it with a stepwise function  $a: [0, 1] \rightarrow \mathbb{R}_+$ , such that  $a(0) = 0$  and for all  $i \in [m]$  and  $x$  in  $(\frac{i-1}{m}, \frac{i}{m}]$  we have  $a(x) = (m \cdot a_i) / (a_1 + \dots + a_m)$ . Further, for each  $x \in [0, 1]$  we set  $A(x) = \int_0^x a(y) dy$ . Note that the normalization in function  $a(\cdot)$  ensures that  $A(1) = 1$ . For two

vectors  $\vec{a} \in \mathbb{R}^s$  and  $\vec{b} \in \mathbb{R}^t$  of possibly different dimensions, we define their *Wasserstein distance* as  $W(\vec{a}, \vec{b}) = \int_0^1 |A(x) - B(x)| dx$ . As  $a(x)$  and  $b(x)$  are stepwise and  $A(x)$  and  $B(x)$  are piecewise linear,  $W(\vec{a}, \vec{b})$  can be computed in polynomial time (assuming we can perform arithmetic operations in polynomial time).

**Frequency Matrices and Positionwise Distance.** Consider an election  $E = (C, V)$ , where  $C = \{c_1, \dots, c_m\}$  and  $V = (v_1, \dots, v_n)$ . A *frequency matrix* of a top-truncated vote  $v \in V$  is an  $m \times m$  matrix  $\text{freq}(v)$  where the entry in the  $i$ -th row and  $j$ -th column is:

$$\text{freq}(v)_{i,j} = \begin{cases} 1 & \text{if } c_j \in C_v^\uparrow \text{ and } v \text{ ranks it } i\text{-th there,} \\ 1/|C_v^\downarrow| & \text{if } c_j \in C_v^\downarrow \text{ and } i > |C_v^\uparrow|, \\ 0 & \text{otherwise.} \end{cases}$$

A frequency matrix of election  $E$  is the average of the frequency matrices of its votes, i.e.,  $\text{freq}(E) = 1/n \sum_{v_i \in V} \text{freq}(v_i)$ . Intuitively,  $\text{freq}(E)_{i,j}$  is the probability that in a randomly selected vote from  $E$  the  $j$ -th candidate is ranked in the  $i$ -th position (where being in the truncated part of a vote means having equal chance of being ranked in any of the truncated positions). Frequency matrices are normalized variants of *position matrices* of Szufa et al. (2020); see also the works of Boehmer et al. (2022a, 2023) (these authors did not consider top-truncated votes; we added this extension). Frequency matrices are bistochastic, i.e., each of their columns and each of their rows sums up to 1.

The Wasserstein distance between two bistochastic matrices,  $X = [\vec{x}_1, \dots, \vec{x}_m]$  and  $Y = [\vec{y}_1, \dots, \vec{y}_m]$ , with  $m$  column vectors each, is the sum of the Wasserstein distances between their (optimally matched) column vectors. Formally:

$$d_W(X, Y) = \min_{\sigma \in \Pi([m], [m])} \frac{1}{m} \sum_{i \in [m]} W(\vec{x}_i, \vec{y}_{\sigma(i)}).$$

Then, the positionwise distance of two equal-sized elections,  $E$  and  $F$ , is the Wasserstein distance of their frequency matrices,  $d_{\text{pos}}(E, F) = d_W(\text{freq}(E), \text{freq}(F))$ . This distance was originally defined by Szufa et al. (2020) using the classic earth mover's distance (EMD) of Rubner, Tomasi, and Guibas (2000), defined for vectors of the same dimension that sum up to the same value. We prefer the Wasserstein distance because it applies to vectors of different dimensions, while being closely related to EMD (in the proposition below,  $\text{emd}(\vec{a}, \vec{b})$  is the EMD distance between vectors and  $\vec{a}$  and  $\vec{b}$ , and is known to be between 0 and  $m - 1$ ; hence  $mW(\vec{a}, \vec{b})$  is its good approximation both for very similar and quite far-off vectors).

**Proposition 2.1.** *For each two  $m$ -dimensional vectors  $\vec{a}$  and  $\vec{b}$  with nonnegative entries that sum up to 1, it holds that  $\max(\frac{1}{2}\text{emd}(\vec{a}, \vec{b}), \text{emd}(\vec{a}, \vec{b}) - 1) \leq mW(\vec{a}, \vec{b}) \leq \text{emd}(\vec{a}, \vec{b})$ .*

Like the isomorphic swap distance, the positionwise distance is invariant to renaming the candidates and reordering the voters, but it differs in that it can assume value 0 even for pairs of nonisomorphic elections. Positionwise distance is normalized in the sense that its largest value is about  $1/3$  (we omit exact calculations).

**Maps of Elections.** A map of elections is a set of elections with distances between each pair of them (called *original distances*). We associate each election with a point in a 2D space so that the Euclidean distances between the points resemble the original ones, using either multidimensional scaling (MDS (Kruskal 1964)) or Kamada-Kawai (KK (Kamada and Kawai 1989)) embedding algorithms.

### 3 Search for More Versatile Distances

Our first goal is to find a satisfying distance  $\hat{d}$  over different-sized, complete elections (as a convention, we will be marking distances that can handle different-sized elections with a “hat” on top). Ideally, we would like  $\hat{d}$  to be an extension of an appealing distance among equal-sized elections, and to put “obviously” identical elections at distance 0. Below we express these requirements formally:

1. We say that  $\hat{d}$  is a *swap extension* if it is a distance and for each two equal-sized/complete elections  $E_1$  and  $E_2$  with  $n$  voters and  $m$  candidates,  $\hat{d}(E_1, E_2) = d_{\text{swap}}(E_1, E_2)$ . We define a *positionwise extension* analogously.
2. We say that  $\hat{d}$  is *ID-consistent* if for all  $p, r, s, q \in \mathbb{N}$ ,  $p, r \geq 3$ , we have  $\hat{d}(\text{ID}_{p,q}, \text{ID}_{r,s}) = 0$ . We define *AN-consistency* and *UN-consistency* analogously. (We consider at least 3 candidates as  $\text{AN}_{2,2} = \text{UN}_{2,2}$ , so without this restriction assuming both AN- and UN-consistency would put all AN and UN elections at distance zero.)

We would like a swap extension or a positionwise extension that is ID-, AN-, and UN-consistent. Naturally, one could think of further conditions, but these are both natural and quite minimal. Yet, even this is too much to ask for.

**Proposition 3.1.** *There is no swap extension nor positionwise extension that simultaneously satisfies ID-, AN- and UN-consistency.*

This means that either we have to give up on at least one of the consistency properties, or on looking for swap/positionwise extensions. We explore both of these possibilities.

#### 3.1 Intuitive Swap/Positionwise Extensions

As far as swap extensions go, one natural idea is that given two elections  $E_1 = (C_1, V_1)$  and  $E_2 = (C_2, V_2)$ , where  $|C_1| < |C_2|$ , we define  $\hat{d}_{\text{swap}}^{\text{tr}}(E_1, E_2)$  as  $d_{\text{swap}}(E'_1, E_2)$ , where  $E'_1$  is equal to  $E_1$  with additional  $|C_2| - |C_1|$  candidates that all voters have in their truncated parts. Unfortunately, this leads to maps where elections with fewer candidates are clustered together, so we lose significant amount of information about them.

**Proposition 3.2.**  *$\hat{d}_{\text{swap}}^{\text{tr}}$  is a swap extension that is neither ID- nor AN- nor UN-consistent.*

Alternatively, we could define  $\hat{d}_{\text{swap}}^{\text{del}}(E_1, E_2)$  to be equal to the expected isomorphic swap distance of elections  $E_1$  and  $E'_2$ , where  $E'_2$  is obtained by deleting  $|C_2| - |C_1|$  candidates from  $E_2$  uniformly at random. However, this is not even a distance as it fails the triangle inequality.

**Proposition 3.3.**  *$\hat{d}_{\text{swap}}^{\text{del}}$  fails triangle inequality.*

One could hope that violations of the triangle inequality are rare and, hence, could be ignored. Unfortunately, based on the experiments, this is not the case, and violations are common. All in all, we were not able to find a satisfying swap extension and we leave looking for one as an open problem. On the positive side, we do identify a natural, UN-consistent positionwise extension that not only applies to different-sized elections, but also seamlessly handles top-truncated votes.

For a matrix  $X = [\vec{x}_1, \dots, \vec{x}_m]$  and an integer  $k \geq 1$ , by  $\text{str}_{mk}(X)$  we denote the matrix obtained from  $X$  by *stretching*, i.e., copying each of its component vectors  $k$  times, so that for each  $i \in [mk]$ , the  $i$ -th vector of  $\text{str}_{mk}(X)$  is  $\vec{x}_{\lceil i/k \rceil}$ . Then, we define the positionwise distance between elections  $E$  and  $F$ —with possibly different numbers of candidates and voters—as  $\hat{d}_{\text{pos}}(E, F) = d_W(\text{str}_s(\text{freq}(E)), \text{str}_s(\text{freq}(F)))$ , where  $s$  is the least common multiple of the numbers of candidates in  $E$  and  $F$ . That is, to obtain  $\hat{d}_{\text{pos}}(E, F)$  we first compute the frequency matrices of  $E$  and  $F$ , then we duplicate their vectors so that both matrices end up with an equal number of columns, and, finally, we match these columns and sum up their Wasserstein distances (recall the definition of the positionwise distance from Section 2; note that here the vectors may be of different dimensions, which is why we chose to use the Wasserstein distance instead of EMD). Truncated votes are handled seamlessly because they are encoded in the frequency matrices. We show that  $\hat{d}_{\text{pos}}$  is indeed a positionwise extension and that it is UN-consistent.

**Theorem 3.4.**  $\hat{d}_{\text{pos}}$  is a positionwise extension that is UN-consistent, but not ID- nor AN-consistent.

Note that Theorem 3.1 does not preclude the existence of a positionwise extension satisfying UN-consistency and either ID- or AN-consistency. Thus, our positionwise distance is not “optimal” in terms of the axioms it satisfies.

### 3.2 Feature Distance and ID/AN/UN-Consistency

In principle, Theorem 3.1 might hold simply because no distance is simultaneously ID-, AN-, and UN-consistent, irrespective of being a swap or a positionwise extensions. We show that this is not the case and at least one such distance exists. To this end, let  $f = (f_1, \dots, f_k)$  be a collection of *features*, i.e., functions that given an election output a value between 0 and 1. For an election  $E$ , its feature vector is  $f(E) = (f_1(E), \dots, f_k(E))$ , and the *feature distance*  $\hat{d}_f$  between elections  $E$  and  $F$  is  $d_f(E, F) = \ell_2(f(E), f(F))$ ; naturally, one could also use  $\ell_1$  or some other distances.<sup>1</sup> For every collection of features  $f$ ,  $\hat{d}_f$  is indeed a distance over different-sized elections, and if the features are defined for top-truncated elections, so is  $\hat{d}_f$ .

Let  $\text{id}(E)$ ,  $\text{an}(E)$ , and  $\text{un}(E)$  be three features such that their value is 0 if the input election is isomorphic to, respectively, some ID, AN, or UN election, and it is 1 otherwise.

<sup>1</sup>For two vectors,  $\vec{a} = (a_1, \dots, a_k)$  and  $\vec{b} = (b_1, \dots, b_k)$ , we define  $\ell_2(\vec{a}, \vec{b}) = \left(\sum_{i=1}^k (a_i - b_i)^2\right)^{1/2}$ .

**Proposition 3.5.** The distance defined by collection  $(\text{id}, \text{an}, \text{un})$  of features is ID-, AN-, and UN-consistent.

While this distance has all the desired consistency properties, it puts all elections that are not isomorphic to ID, AN, or UN at distance zero and, hence, is not very useful. Next we develop a feature distance that implements a similar idea, but in a more sophisticated way. To this end, we focus on evaluating diversity, agreement, and polarization among the votes (indeed, UN captures ideal diversity, ID ideal agreement, and AN—polarization). Let  $E = (C, V)$  be an election. The agreement for candidates  $a, b \in C$  is:

$\alpha(a, b) = \max(|N_E(a \succ b) - N_E(b \succ a)|, N_E(a \sim b)) / |V|$ . Intuitively,  $|N_E(a \succ b) - N_E(b \succ a)| / |V|$  captures the agreement when voters lean toward strict preference over  $a$  and  $b$ , and  $N_E(a \sim b) / |V|$  reflects the agreement when most of the voters put both  $a$  and  $b$  in the truncated parts of their votes. The agreement index of an election  $E = (C, V)$  is an average of agreements for all pairs of candidates, i.e.,  $A(E) = \sum_{\{a, b\} \subseteq C} \alpha(a, b) / \binom{|C|}{2}$ . This definition is a natural extension of the agreement index studied for complete elections by Alcalde-Unzu and Vorsatz (2013), Hashemi and Endriss (2014), and Can, Ozkes, and Storcken (2015). Note that these papers use other names and interpretations for this index—we follow the approach of Faliszewski et al. (2023).

Regarding diversity and polarization, we also follow Faliszewski et al. (2023), but with a few changes. For each integer  $i$ , let the empirical  $i$ -Kemeny score of election  $E$  be:

$$\text{emk}_i(E) = \min_{v_1, \dots, v_i \in V} \left( \sum_{v \in V} (\min_{j \in [i]} \text{swap}(v, v_j)) \right).$$

That is, to compute  $\text{emk}_i(E)$ , we seek  $i$  votes from the election so that the sum of the swap distances of each vote in  $E$  to the closest selected one is minimized. E.g.,  $\text{emk}_1(E)$  is an approximation of the classic Kemeny score (Kemeny 1959). To normalize  $\text{emk}_i(E)$ , we divide by its maximal possible value, i.e.,  $1/2 \cdot |V| \cdot \binom{|C|}{2}$ . We define the diversity and polarization indices as:

$$D(E) = \frac{2}{5} \sum_{i=1}^5 \text{emk}_i(E) / (|V| \cdot \binom{|C|}{2}),$$

$$P(E) = 2 \cdot (\text{emk}_1(E) - \text{emk}_2(E)) / (|V| \cdot \binom{|C|}{2}).$$

The latter is simply an approximation of the polarization index introduced by Faliszewski et al. (2023) and the former is a heuristic built on top of their diversity index; we chose the constant 5 as our initial experiments have shown that it captures the same notion as their approach, and it allows for fast computation; in general, computing  $\text{emk}_i(E)$  is intractable (Faliszewski et al. 2023), so we approximate it using their local search approach.

We prove that for every  $i$ , the value of the empirical  $i$ -Kemeny score of the uniformity election converges to its maximal value as the number of candidates grows.

**Proposition 3.6.** For every constant  $i \in \mathbb{N}$ , it holds that  $\lim_{m \rightarrow \infty} \text{emk}_i(\text{UN}_{m, m!}) = 1/2 \cdot m! \cdot \binom{m}{2}$ .

This gives the following sanity check (arrows mean convergence as the number of candidates grows):

$$D(\text{ID}) = 0, \quad A(\text{ID}) = 1, \quad P(\text{ID}) = 0,$$

$$D(\text{UN}) \rightarrow 1, \quad A(\text{UN}) = 0, \quad P(\text{UN}) \rightarrow 0,$$

$$D(\text{AN}) = 1/5, \quad A(\text{AN}) = 0, \quad P(\text{AN}) = 1.$$

These results are intuitive as in ID all the voters agree, UN is most diverse, and AN is most polarized. The DAP distance, denoted  $\hat{d}_{\text{dap}}$ , is a feature distance that uses  $D$ ,  $A$ , and  $P$  as the features. We see that DAP is ID-consistent and AN-consistent, but not UN-consistent (but it satisfies this property in an approximate sense—the distance between two UN elections with different numbers of candidates gets smaller and smaller as the numbers of candidates in these elections increase).

**Proposition 3.7.**  $\hat{d}_{\text{dap}}$  is ID-consistent and AN-consistent, but is not UN-consistent.

While our diversity feature may appear somewhat ad hoc, we believe that it captures the intuitive notion of diversity among votes and our results are robust to tweaking it. Indeed, in Section 4.2 we find strong correlation between the DAP distance and the swap one (which implicitly relies on diversity analysis (Faliszewski et al. 2023)).

### 3.3 Positionwise Distance Versus DAP

Positionwise distance and DAP vary in several significant ways. Foremost, the positionwise distance deals with different numbers of candidates by, effectively, creating their virtual copies, so that the elections it analyzes look as if they were equal-sized (this process is hidden in computing the Wasserstein distance and in stretching the matrices). On the other hand, DAP identifies structural properties of the elections (diversity, agreement, and polarization) and rescales them to a common denominator, so that different-sized elections can be compared on common grounds.

Second, the two distances treat top-truncated votes differently. DAP inherits its approach from the swap distance that its features are based on (the agreement index is similar in this respect): If a voter puts some candidates in the truncated part, then DAP assumes that he or she sees them as equally bad. In contrast, the positionwise distance assumes that the voter can rank them, but chose not to report it, so the distance assumes a uniform distribution over possible completions.

## 4 Maps of Synthetic Datasets and Evaluation

Our next goal is to understand how the positionwise and DAP distances behave in practice. To this end, we form and analyze maps of synthetic elections, and we evaluate how the distances between elections change as we vary either their size or their level of truncation. First, we describe our data.

### 4.1 Datasets

Our *basic dataset* consists of 326 complete elections with 8 candidates and 96 voters each, and is nearly identical to the one used by Faliszewski et al. (2023) (in particular, we chose the same numbers of candidates and voters as they did). The main part of the dataset consists of elections generated according to the impartial culture (IC), normalized Mallows (Mallows 1957; Boehmer et al. 2021), Pólya-Eggenberger urn (Berg 1985; McCabe-Dansted, Pritchard, and Slinko 2008), and Euclidean models (see, e.g., the work of Enelow and Hinich (1984)). Under impartial culture, we draw each vote uniformly at random. The normalized Mallows model is similar but the votes are clustered around a

given central one (the strength of this clustering is controlled by parameter  $\text{norm-}\phi \in [0, 1]$ , the higher the value the less concentrated are the votes; see the work of Boehmer, Faliszewski, and Kraiczy (2023) for a discussion of this model). The urn model generates elections with clusters of identical votes (the larger its parameter of contagion  $\alpha \geq 0$  is, the fewer clusters there are, each containing more votes (Faliszewski et al. 2023)). In the Euclidean models, candidates and voters are points in some Euclidean space and voters prefer the closer candidates (we draw the points uniformly from a unit hypercube or hypersphere of a given dimension; for 1-, 2-, and 3- dimensional hypercubes we refer to the models as Interval, Square, and Cube; for 1- and 2- dimensional hyperspheres we refer to them as Circle and Sphere). The dataset also includes elections generated using statistical cultures that yield single-peaked (Black 1958), SPOC (Peters and Lackner 2020), and group-separable (Inada 1964, 1969) elections. Finally, we add ID, AN, and an approximation of UN elections together with artificial elections forming paths between these three on our maps (which include ST election in which each voter ranks the same half of the candidates on top, but otherwise the votes are chosen uniformly at random).

We generated the *size-oriented dataset* in the same way as the basic one, except that for each culture we partitioned its elections into four groups, with either 8 or 16 candidates and either 96 or 192 voters. We obtain top-truncated elections from complete ones by using the following methods:

1. Top- $k$  truncation removes from each vote the candidates below position  $k$ . Such data appears, e.g., in Preflib in the sushi dataset, where people rank their top 10 sushi types out of 100 available ones (Kamishima 2003) (see Preflib file 00014-00000002.so.i).
2. Random cut truncation is parameterized by probability  $p$ . For each vote, we consider its candidates from top to bottom and with probability  $1 - p$  we stop the process, truncating the vote after the current candidate. Some of the political elections follow a similar pattern, e.g., UK Labour Party leadership election (Riley, Ryan, and Smith 2010) (see Preflib file 00030-00000001.so.i).
3. Random drop truncation moves each candidate in each vote to the truncated part, independently, with probability  $p$ . This imitates sport elections—such as those for Formula 1—where each player fails to finish a given competition with some probability.

To form the *comprehensive dataset*, we took the size-oriented one and for each group of elections (of a given size, generated using a given statistical culture) we left the first half of the elections in the group intact, we applied the top- $k$  truncation to the next quarter of them, and we applied random cut truncation to the last quarter. We chose the truncation parameters so that, in expectation, each voter ranked half of the candidates. We generated the *truncation-oriented dataset* in the same way, but starting from the basic dataset. We also generated a *random drop dataset*, but we omitted it from the experiments as its elections have very different nature (we analyze them in Section F).

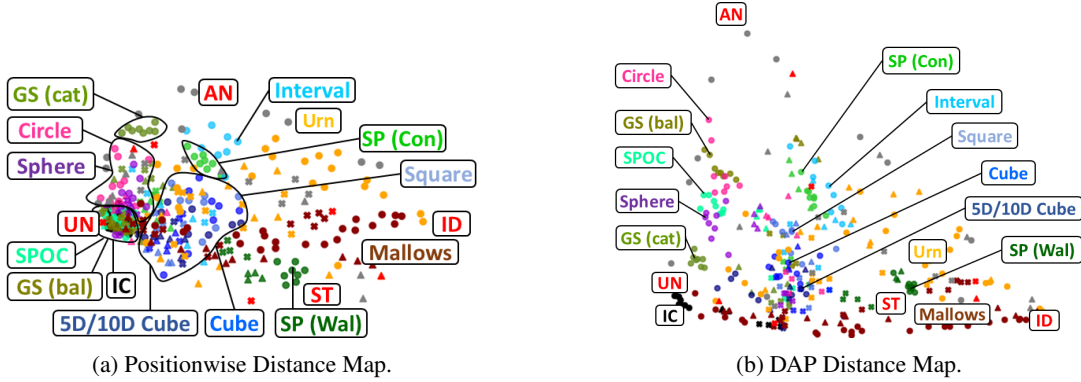


Figure 2: Maps of elections created using the positionwise and DAP distances, for the truncation-oriented datasets. Top- $k$  truncated elections are marked with triangles, random-cut truncated ones with crosses, and complete ones with circles.

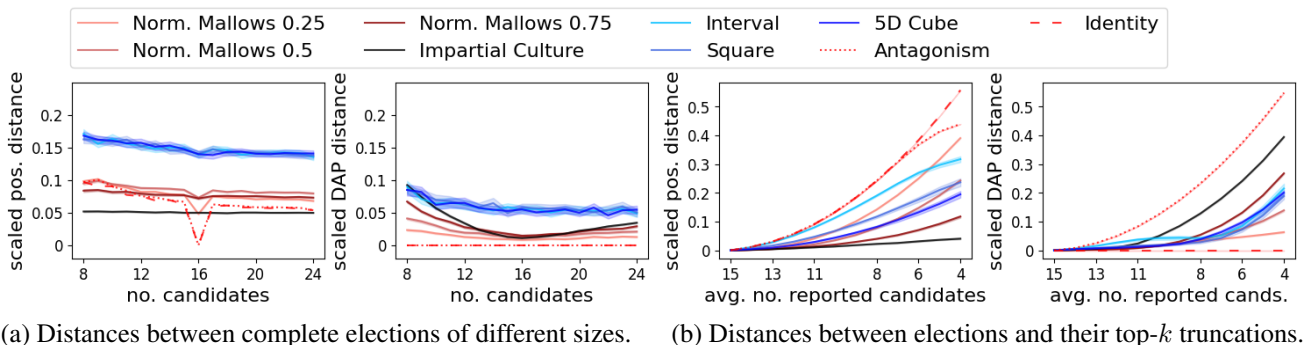


Figure 3: Plots (a) show average distance from size-16 elections to different-sized, complete elections from the same culture, as a fraction of the maximum distance in our dataset (positionwise distance on the left, DAP distance on the right). Plots (b) show average distance from a complete election to its top- $k$  truncation, as a fraction of the maximum distance in our dataset (positionwise distance on the left, DAP distance on the right).

## 4.2 Maps of Elections

We show maps for the truncation-based dataset obtained using our two distances in Figure 2, with the KK embedding (Kamada and Kawai 1989) used for the positionwise distance, and MDS (Kruskal 1964) used for DAP. The maps for size-based and comprehensive datasets can be found in Section G.

The map obtained using the positionwise distance is similar to that of the basic dataset (shown in Figure 1a) and the map obtained using the DAP distance resembles the map of the basic dataset obtained using the swap distance (Figure 1b), albeit with some level of degradation. For the positionwise map, the truncated elections tend to be closer to UN than their complete counterparts and for DAP we see a cluster of random-cut elections one-third of a way between UN and ID elections. Unfortunately, if we used random drop truncation (with dropping probability of 0.5) then all thus-generated elections would form a single cluster in the vicinity of UN. One explanation for this is that random drop affects the internal structure of elections very strongly. For example, in the  $AN_8$  election only two candidates are ever ranked first, but with random drop truncation every candidate has a nonnegligible probability of being ranked first.

Thus, analyzing random-drop elections is particularly difficult. Still, the maps indicate that, on the high level, both distances give intuitive, reasonable results.

## 4.3 Varying Election Sizes Truncation Level

Next, we evaluate the robustness of our distances in a more quantitative way. First, we analyze their ability to recognize similar elections with different numbers of candidates. To this end, for each of several statistical cultures (IC, normalized Mallows model with norm- $\phi \in \{0.25, 0.5, 0.75\}$ , and 1D/2D/5D Euclidean models with points distributed uniformly on unit hypercubes) and for each integer  $m$  between 8 and 24, we generated 100 pairs of elections, each with 192 voters, where one election in the pair had  $m$  candidates and the other one had 16, and we computed their average distance (normalized by the largest distance that occurred in the datasets from Section 4.1, i.e., an approximate diameter of the election space; consequently, the results for positionwise and DAP are on the same scale). We report the results in Figure 3(a), the shaded areas show 95% confidence intervals (we also included ID and AN elections in the plot; IC can be seen as an approximation of UN). Ideally, we would like our plots to consist of flat lines, close to zero. This would

mean that a given distance can recognize structural similarities between elections generated in the same way, even if these elections have different numbers of candidates. Hence, in our view DAP performs better as its scaled values are significantly smaller, even if the results for Mallows are less flat (as the Mallows and IC lines are increasing, the reader may worry what happens for even more candidates; in short, they increase slowly, with IC reaching about 10% of the diameter for the case of 100 candidates). It is reassuring that for DAP the plots for ID and AN are flat at value zero (as DAP is ID- and AN-consistent), and for positionwise the plot for IC is flat and close to zero (as positionwise is UN-consistent and IC elections approximate UN).

To analyze the influence of truncation, for each of the cultures from the previous experiment we generated 25 elections with 16 candidates and 192 voters, and applied each of our truncation methods to each of them changing the parameter to obtain varying levels of vote completeness. For each truncated election, we computed its distance from the original, complete one (and normalized it as previously). In Figure 3(b) we plot the average of these values, for the case of top- $k$  truncation; shaded area shows 95% confidence interval. We see that if the voters rank at least half of the candidates, then the average distance of the truncated election from its complete variant is (a) less than 20% of the diameter for the positionwise distance (indeed, even less than 10% for most of the cultures), and (b) less than 5% of the diameter for DAP (except for AN and IC elections, where it is  $\leq 30\%$  and  $\leq 15\%$  of the diameter, respectively). Thus, both distances handle truncated data well, but DAP has an advantage (however, for the other truncation types DAP and positionwise perform similarly to each other). Overall, the experiments point to DAP.

## 5 Map of Preflib

Last but not least, we present the *Map of Preflib*, obtained using the DAP distance (we offer more in-depth analysis in Section H). Boehmer et al. (2021) already tried putting Preflib elections on the map, but their approach was limited to elections with 10 candidates and 100 complete votes, obtained by involved preprocessing. We use raw, unprocessed elections from Preflib, with the number of candidates ranging from 3 to  $\approx 2\,600$  and the number of voters from 4 to  $\approx 64\,000$ . We also use more elections, as Preflib was extended since their work.

We show our map in Figure 4: Each black dot represents a single election from Preflib, while large pale discs represent elections generated synthetically (much more detailed analysis is available in the extended version of the paper). We find that most of the Preflib elections fall between Euclidean ones (with uniform distribution of candidate and voter points inside a unit hypercube of between 2 and 10 dimensions), Mallows elections (with norm- $\phi$  values in the range  $[0.2, 0.7]$ ), and urn elections (with contagion parameter in the range  $[0.2, 0.5]$ , or  $[0.2, 2]$  if one wants to include elections with large clusters of identical votes; similar elections happen in Preflib, but are more rare). This motivates the use of these models and parameter ranges to generate

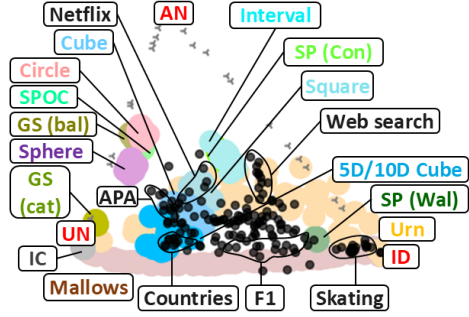


Figure 4: Map of Preflib elections (black dots) in addition to the synthetic ones (large pale discs), obtained using the DAP distance.

realistic-looking data using only the few best-known statistical cultures. Some previous papers, including those of Boehmer et al. (2021) and Faliszewski et al. (2023), argued that the urn model does not generate realistic elections but our results counter this. That said, we also see an area with many Preflib elections, but no elections from our statistical cultures (black dots over white background). It would be interesting to find statistical cultures that do cover this space.

Next, let us analyze the locations of the Preflib elections with respect to ID, UN, and AN. Foremost, we see that the area near AN is empty and, hence, Preflib elections are not strongly polarized (the same effect was visible in the map of Boehmer et al. (2021)). Some elections that (weakly) stand out in this respect include those in the WebSearch dataset (but they include only 4 votes each and, hence, are very particular), some Netflix elections (where each voter ranks the same 3 or 4 movies, so some level of disagreement is expected) and some APA elections (which involve 5 candidates for the president of the American Psychological Association, with some tension between “academics” and “clinicians”). Elections from the (Figure) Skating, Formula 1, and Countries datasets represent the other extreme and are located between ID and UN, close to the Mallows elections. These locations are quite natural: Indeed, we expect the judges in figure skating, who evaluate the same performances, conducted on the same day, to be correlated, and we expect Formula 1 races that happen over the course of a season to be more varied.

## 6 Summary

We found that the DAP distance is an interpretable, scalable way of assessing similarity between different-sized/top-truncated elections, suitable to form a map of (a fragment of) Preflib. By analyzing this map, we were able to draw a number of conclusions, including the parameters for Mallows, urn, and Euclidean models that yield realistic elections.

Nevertheless, we believe that there is no one-fit-all method for creating maps, and different applications may call for different approaches. Thus, considering different distances, including but not limited to feature distances with different set of features, and developing arguments for their usefulness might be a fruitful direction for future research.

## Acknowledgements

This project has received funding from the European Research Council (ERC) under the European Union's Horizon 2020 research and innovation programme (grant agreement No 101002854), from the French government under management of Agence Nationale de la Recherche as part of the "Investissements d'avenir" program, reference ANR-19-P3IA-0001 (PRAIRIE 3IA Institute), and from the European Union under the project Robotics and advanced industrial production (reg. no. CZ.02.01.01/00/22\_008/0004590). J. Mertlová acknowledges the additional support of the Faculty of Information Technology of the Czech Technical University in Prague via the Výzkumné léto (VýLeT) project. S. Szufa was supported by the Foundation for Polish Science (FNP). T. Wąs was partially supported by EPSRC under grant EP/X038548/1.



## References

Alcalde-Unzu, J.; and Vorsatz, M. 2013. Measuring the Closeness of Preferences: An Axiomatic Analysis. *Social Choice and Welfare*, 41(4): 965–988.

Baumeister, D.; Faliszewski, P.; Lang, J.; and Rothe, J. 2012. Campaigns for Lazy Voters: Truncated Ballots. In *Proceedings of AAMAS-2012*, 577–584.

Ben-Naim, E. 2010. Mixing of diffusing particles. *Physical Review E*, 82(6): 061103.

Berg, S. 1985. Paradox of Voting Under an Urn Model: The Effect of Homogeneity. *Public Choice*, 47(2): 377–387.

Black, D. 1958. *The Theory of Committees and Elections*. Cambridge University Press.

Boehmer, N.; Bredereck, R.; Elkind, E.; Faliszewski, P.; and Szufa, S. 2022a. Expected Frequency Matrices of Elections: Computation, Geometry, and Preference Learning. In *Proceedings of NeurIPS-2022*.

Boehmer, N.; Bredereck, R.; Faliszewski, P.; Niedermeier, R.; and Szufa, S. 2021. Putting a Compass on the Map of Elections. In *Proceedings of IJCAI-2021*, 59–65.

Boehmer, N.; Cai, J.-Y.; Faliszewski, P.; Fan, A.; Janeczko, L.; Kaczmarczyk, A.; and Wąs, T. 2023. Properties of Position Matrices and Their Elections. In *Proceedings of AAAI-2023*, 5507–5514.

Boehmer, N.; Faliszewski, P.; and Kraiczy, S. 2023. Properties of the Mallows Model Depending on the Number of Alternatives: A Warning for an Experimentalist. In *Proceedings of ICML-2023*.

Boehmer, N.; Faliszewski, P.; Niedermeier, R.; Szufa, S.; and Wąs, T. 2022b. Understanding Distance Measures Among Elections. In *Proceedings of IJCAI-2022*, 102–108.

Boehmer, N.; and Schaar, N. 2023. Collecting, Classifying, Analyzing, and Using Real-World Ranking Data. In *Proceedings of AAMAS-2023*, 1706–1715.

Borodin, A.; Halpern, D.; Latifian, M.; and Shah, N. 2022. Distortion in Voting with Top-t Preferences. In *Proceedings of IJCAI-2022*, 116–122.

Can, B.; Ozkes, A. I.; and Storcken, T. 2015. Measuring Polarization in Preferences. *Mathematical Social Sciences*, 78: 76–79.

Conitzer, V. 2009. Eliciting Single-Peaked Preferences Using Comparison Queries. *Journal of Artificial Intelligence Research*, 35: 161–191.

Enelow, J.; and Hinich, M. 1984. *The Spatial Theory of Voting: An Introduction*. Cambridge University Press.

Faliszewski, P.; Kaczmarczyk, A.; Sornat, K.; Szufa, S.; and Wąs, T. 2023. Diversity, Agreement, and Polarization in Elections. In *Proceedings of IJCAI-2023*, 2684–2692.

Faliszewski, P.; Skowron, P.; Slinko, A.; Szufa, S.; and Talmor, N. 2019. How Similar Are Two Elections? In *Proceedings of AAAI-2019*, 1909–1916.

Hashemi, V.; and Endriss, U. 2014. Measuring Diversity of Preferences in a Group. In *Proceedings of ECAI-2014*, 423–428.

Inada, K. 1964. A Note on the Simple Majority Decision Rule. *Econometrica*, 32(32): 525–531.

Inada, K. 1969. The Simple Majority Decision Rule. *Econometrica*, 37(3): 490–506.

Kamada, T.; and Kawai, S. 1989. An Algorithm for Drawing General Undirected Graphs. *Information Processing Letters*, 31(1): 7–15.

Kamishima, T. 2003. Nantonac Collaborative Filtering: Recommendation Based on Order Responses. In *Proceedings of KDD-2003*, 583–588.

Karpov, A. 2019. On the number of group-separable preference profiles. *Group Decision and Negotiation*, 28(3): 501–517.

Kemeny, J. 1959. Mathematics Without Numbers. *Daedalus*, 88: 577–591.

Kilgour, D. M.; Grégoire, J.-C.; and Foley, A. M. 2020. The prevalence and consequences of ballot truncation in ranked-choice elections. *Public Choice*, 184: 197–218.

Kruskal, J. 1964. Multidimensional Scaling by Optimizing Goodness of Fit to a Nonmetric Hypothesis. *Psychometrika*, 29(1): 1–27.

Mallows, C. 1957. Non-null ranking models. *Biometrika*, 44: 114–130.

Mattei, N.; and Walsh, T. 2013. PrefLib: A Library for Preferences. In *Proceedings of ADT-2013*, 259–270.

McCabe-Dansted, J.; Pritchard, G.; and Slinko, A. 2008. Approximability of Dodgson's Rule. *Social Choice and Welfare*, 31(2): 311–330.

McCabe-Dansted, J.; and Slinko, A. 2006. Exploratory Analysis of Similarities Between Social Choice Rules. *Group Decision and Negotiation*, 15: 77–107.

Peters, D.; and Lackner, M. 2020. Preferences Single-Peaked on a Circle. *Journal of Artificial Intelligence Research*, 68: 463–502.

Riley, J.; Ryan, I.; and Smith, W. 2010. The Election, by Instant Runoff Voting, of UK Labour Party Leader in late-September 2010. <https://rangevoting.org/LabourUK2010.html>.

Rubner, Y.; Tomasi, C.; and Guibas, L. 2000. The Earth Mover’s Distance as a Metric for Image Retrieval. *International Journal of Computer Vision*, 40(2): 99–121.

Szufa, S.; Faliszewski, P.; Skowron, P.; Slinko, A.; and Talmon, N. 2020. Drawing a Map of Elections in the Space of Statistical Cultures. In *Proceedings of AAMAS-2020*, 1341–1349.

Tomlinson, K.; Ugander, J.; and Kleinberg, J. 2023. Ballot length in instant runoff voting. In *Proceedings of AAAI-2023*, 5841–5849.

Walsh, T. 2015. Generating Single Peaked Votes. Technical Report arXiv:1503.02766 [cs.GT], arXiv.org.

## A Relation Between EMD and Wasserstein Distances

The original positionwise distance, as defined by Szufa et al. (2020) used earth mover's distance (EMD) between vectors and not Wasserstein's, as we do. In this section we argue that the difference between the two distances is small and bounded (for the case of vectors of the same dimension).

First, let us recall definitions of the EMD and  $\ell_1$  distances. Given two vectors,  $\vec{a} = [a_1, \dots, a_m]$  and  $\vec{b} = [b_1, \dots, b_m]$ , their  $\ell_1$  distance is:

$$\ell_1(\vec{a}, \vec{b}) = |a_1 - b_1| + |a_2 - b_2| + \dots + |a_m - b_m|.$$

If, additionally, their entries are nonnegative and sum up to 1, then their EMD distance, denoted  $\text{emd}(\vec{a}, \vec{b})$ , is the smallest total cost of transforming  $\vec{a}$  into  $\vec{b}$  through operations of the following form: Given  $i, j \in [m]$  and a number  $\delta \leq a_i$ , we can move value  $\delta$  from position  $i$  in  $\vec{a}$  to position  $j$  at cost  $\delta \cdot |i - j|$ . In other words, we view vector  $\vec{a}$  as a collection of  $m$  buckets, where each bucket  $i$  contains  $a_i$  amount of sand. We can move the sand between the buckets, but each such operation costs proportionally to the distance between the buckets and the amount of sand moved. It is also well-known that we can express  $\text{emd}(\vec{a}, \vec{b})$  using the  $\ell_1$  distance and the notation where for each  $i \in [m]$ ,  $\hat{a}_i$  and  $\hat{b}_i$  mean  $a_1 + \dots + a_i$  and  $b_1 + \dots + b_i$ , respectively (Rubner, Tomasi, and Guibas 2000):

$$\text{emd}(\vec{a}, \vec{b}) = |\hat{a}_1 - \hat{b}_1| + \dots + |\hat{a}_m - \hat{b}_m|.$$

**Proposition A.1.** *For each two vectors,  $\vec{a} = [a_1, \dots, a_m]$  and  $\vec{b} = [b_1, \dots, b_m]$ , with nonnegative entries that sum up to 1, it holds that:*

$$\text{emd}(\vec{a}, \vec{b}) - 1 \leq m \cdot W(\vec{a}, \vec{b}) \leq \text{emd}(\vec{a}, \vec{b})$$

*Proof.* Let  $\vec{a}$  and  $\vec{b}$  be as in the statement of the proposition. Following the definition of their Wasserstein's distance from Section 2, we consider their associated functions  $a(\cdot)$ ,  $b(\cdot)$ ,  $A(\cdot)$ , and  $B(\cdot)$ . In particular, we observe that for each  $i \in [m]$  and each  $x \in [\frac{i-1}{m}, \frac{i}{m}]$  we have:

$$a(x) = a_i m, \quad b(x) = b_i m.$$

Since  $A(x) = \int_0^x a(y) dy$  and  $B(x) = \int_0^x b(y) dy$ , for each  $i \in [m]$  and each  $x \in [\frac{i-1}{m}, \frac{i}{m}]$  we also have:

$$A(x) = \hat{a}_{i-1} + (x - \frac{i-1}{m}) a_i m, \text{ and}$$

$$B(x) = \hat{b}_{i-1} + (x - \frac{i-1}{m}) b_i m,$$

which, after basic calculations, gives:

$$A(x) = \hat{a}_i - (\frac{i}{m} - x) a_i m, \text{ and}$$

$$B(x) = \hat{b}_i - (\frac{i}{m} - x) b_i m.$$

Now we are ready to calculate  $W(\vec{a}, \vec{b})$ . We have:

$$\begin{aligned} W(\vec{a}, \vec{b}) &= \int_0^1 |A(x) - B(x)| dx \\ &= \sum_{i=1}^m \left( \int_{\frac{i-1}{m}}^{\frac{i}{m}} |A(x) - B(x)| dx \right) \end{aligned} \quad (1)$$

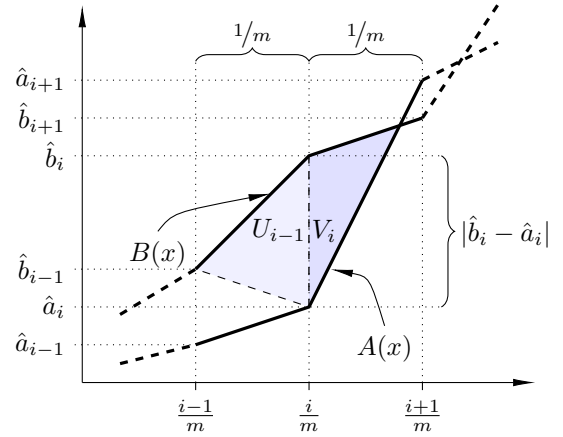


Figure 5: Illustration of the proof that  $W(\vec{a}, \vec{b}) \leq \frac{1}{m} \text{emd}(\vec{a}, \vec{b})$ .

For each  $i \in [m]$ , we express the integral under the sum as:

$$\int_{\frac{i-1}{m}}^{\frac{i}{m}} |\hat{a}_i - \hat{b}_i - (\frac{i}{m} - x)(b_i - a_i)m| dx, \quad (2)$$

which is greater or equal to the following expression (see explanations below):

$$\begin{aligned} &\int_{\frac{i-1}{m}}^{\frac{i}{m}} |\hat{a}_i - \hat{b}_i| dx - \int_{\frac{i-1}{m}}^{\frac{i}{m}} |(\frac{i}{m} - x)(b_i - a_i)m| dx, \\ &= \frac{1}{m} |\hat{a}_i - \hat{b}_i| - \frac{1}{2m} |b_i - a_i|. \end{aligned}$$

The fact that the first expression in the above equality is smaller or equal than (2) follows from the fact that for each  $\alpha, \beta \in \mathbb{R}$ ,  $|\alpha + \beta| \geq |\alpha| - |\beta|$ , and the next equality follows by computing the integrals (in particular,  $\int_{\frac{i-1}{m}}^{\frac{i}{m}} |(\frac{i}{m} - x)(b_i - a_i)m| dx$  is the area of a triangle with height  $1/m$  and base equal to  $|b_i - a_i|$ ).

Altogether, after substituting these calculations into (1), we obtain that  $W(\vec{a}, \vec{b})$  is greater or equal to:

$$\sum_{i=1}^m \frac{1}{m} |\hat{a}_i - \hat{b}_i| - \frac{|a_i - b_i|}{2m} = 1/m \left( \text{emd}(\vec{a}, \vec{b}) - \frac{1}{2} \ell_1(\vec{a}, \vec{b}) \right).$$

By observing that  $\ell_1(\vec{a}, \vec{b}) \leq 2$ , we have the first inequality from the statement of the proposition.

Next, we show that  $W(\vec{a}, \vec{b}) \leq \frac{1}{m} \text{emd}(\vec{a}, \vec{b})$ . Geometric interpretation of  $W(\vec{a}, \vec{b})$  is that it is the area between functions  $A(x)$  and  $B(x)$ , for  $x \in [0, 1]$ . From the preceding arguments, we know that for each  $i \in [m]$ ,  $A(\frac{i}{m}) = \hat{a}_i$  and  $B(\frac{i}{m}) = \hat{b}_i$ . Further, both functions are linear within each interval  $[\frac{i-1}{m}, \frac{i}{m}]$ . We partition the area between functions  $A(x)$  and  $B(x)$  into  $2m$  triangles as follows (see Figure 5 for illustration): For each  $i \in [m]$ , we form triangle  $U_{i-1}$  connecting points  $(\frac{i-1}{m}, \hat{a}_{i-1})$ ,  $(\frac{i}{m}, \hat{b}_i)$  and either  $(\frac{i-1}{m}, \hat{b}_{i-1})$ , if  $A(x)$  and  $B(x)$  do not intersect in the interval  $[\frac{i-1}{m}, \frac{i}{m}]$ , or their intersection point in that interval, if they do. Similarly, we form triangle  $V_i$  connecting points

$(\frac{i}{m}, \hat{a}_i)$ ,  $(\frac{i}{m}, \hat{b}_i)$  and either  $(\frac{i+1}{m}, \hat{a}_{i-1})$ , if  $A(x)$  and  $B(x)$  do not intersect in the interval  $[\frac{i}{m}, \frac{i+1}{m}]$ , or their intersection point in that interval, if they do (we take  $V_m$  to be an empty triangle). Note that together the area of these triangles is equal to  $W(\vec{a}, \vec{b})$ . Further, one can easily verify that for each  $i \in [m]$ , the area of each of the triangles  $U_{i-1}$  and  $V_i$  is bounded by  $\frac{1}{2} \cdot \frac{1}{m} |\hat{a}_i - \hat{b}_i|$ . Consequently, we have  $W(\vec{a}, \vec{b}) \leq \sum_{i=1}^m \frac{1}{m} |\hat{a}_i - \hat{b}_i| = \frac{1}{m} \text{emd}(\vec{a}, \vec{b})$ .  $\square$

By a careful analysis of the second part of the above proof, we also obtain the following corollary.

**Corollary A.2.** *For each two vectors,  $\vec{a} = [a_1, \dots, a_m]$  and  $\vec{b} = [b_1, \dots, b_m]$ , with nonnegative entries that sum up to 1, it holds that:*

$$\frac{1}{2} \text{emd}(\vec{a}, \vec{b}) \leq m \cdot W(\vec{a}, \vec{b}) \leq \text{emd}(\vec{a}, \vec{b})$$

In essence, it follows by observing that if we replaced function  $A(x)$  with  $A'(x) = \min(A(x), B(x))$  and function  $B(x)$  with  $B'(x) = \max(A(x), B(x))$  then we would have:

$$\text{emd}(\vec{a}, \vec{b}) = \int_0^1 |A'(x) - B'(x)| dx$$

This integral is at most twice as large as the  $\int_0^1 |A(x) - B(x)| dx$ . Indeed, if for a given  $i \in [m]$  and all  $x \in [i-1/m, i/m]$  we have that  $A(x) \leq B(x)$ , then the two integrals are equal for this range of  $x$ . If, on the other hand, the graphs of functions  $A(x)$  and  $B(x)$  cross, then  $\int_{i-1/m}^{i/m} |A'(x) - B'(x)| dx \leq 2 \int_{i-1/m}^{i/m} |A(x) - B(x)| dx$ . This follows because the area of a trapezoid is at most twice as large as the joint area of the two triangles formed by its bases and diagonals.

Jointly, Theorem A.1 and Theorem A.2 say that the Wasserstein distance is similar to EMD both when the input vectors are close to each other (in which case Theorem A.2 gives a more accurate bound) and when they are far away (in which case Theorem A.1 kicks in).

Finally, we observe that the bound in Theorem A.2 is tight, but the one in Theorem A.1 can potentially be improved. To this end, let us fix a positive integer  $m$  and consider the following two vectors of dimension  $2m+1$ :

$$\begin{aligned} \vec{a} &= [\frac{1}{2m}, 0, \frac{1}{m}, 0, \frac{1}{m}, \dots, 0, \frac{1}{m}, 0, \frac{1}{2m}] \\ \vec{b} &= [0, \frac{1}{m}, 0, \frac{1}{m}, \dots, 0, \frac{1}{m}, 0] \end{aligned}$$

We can see that  $\text{emd}(\vec{a}, \vec{b}) = 1$  (in essence, to obtain  $\vec{b}$  from  $\vec{a}$ , both  $\frac{1}{2m}$  entries need to move to their neighbors in full, whereas each  $\frac{1}{m}$  entry needs to move half of its value to the left and half of its value to the right). Careful computation also shows that  $(2m+1) \cdot W(\vec{a}, \vec{b})$  is equal to:

$$\begin{aligned} (2m+1) \cdot \left( \frac{1}{2m(2m+1)} + (2m-1) \frac{1}{4m(2m+1)} \right) \\ = \frac{1}{2m} + (2m-1) \frac{1}{4m} = \frac{2m+1}{4m} = \frac{1}{2} + \frac{1}{4m}. \end{aligned}$$

As  $m$  goes to infinity, this value approaches  $\frac{1}{2}$ , i.e., half of the value of the EMD distance.

## B Statistical Cultures and Our Dataset

We first describe the statistical cultures that we use and then we give the details of our synthetic datasets.

### B.1 Statistical Cultures

All the statistical cultures that we consider generate complete elections. Hence, whenever below we speak of a vote, we mean a complete one.

**Impartial Culture.** Under impartial culture (IC) we generate elections vote-by-vote, drawing the preferences of each voter uniformly at random from the set of all possible ones.

**(Normalized) Mallows Model.** Mallows model is similar to IC in that we also generate votes one-by-one, but instead of drawing them uniformly at random, we use a distribution clustered around a given central vote. Formally, if  $u$  is the *central vote* and  $\phi \in [0, 1]$  is the so-called *parameter of dispersion*, then the probability of generating vote  $v$  is proportional to  $\phi^{\text{swap}(u, v)}$  (Mallows 1957). However, instead of using the parameter  $\phi$  directly, we use its normalized variant called *norm- $\phi$*   $\in [0, 1]$  and introduced by Boehmer et al. (2021). Formally, given a value of *norm- $\phi$*  and the number  $m$  of candidates that we consider, we use a value of  $\phi$  such that the expected swap distance between the votes that the Mallows model generates and the central one is equal to:

$$\text{norm-}\phi \cdot \frac{m(m-1)}{4}.$$

Intuitively,  $\frac{m(m-1)}{4}$  is half of the maximum swap distance between two preference orders over  $m$  candidates, so setting *norm- $\phi$*  = 1 leads to generating maximally diverse votes (indeed, in this case the model is equivalent to IC), whereas setting *norm- $\phi$*  = 0 requires all generated votes to be identical to the central one. Boehmer et al. (2021) and Boehmer, Faliszewski, and Kraiczy (2023) argue how choosing the *norm- $\phi$*  values in between 0 and 1 leads to smooth transition between these two extremes, independent of the number of candidates (without the normalization the transition becomes more and more abrupt as the number of candidates grows).

**Polya-Eggenberger Urn Model.** The urn model uses the *parameter of contagion*  $\alpha \geq 0$ . The model was introduced by Berg (1985), but the parameterization that we use is due to McCabe-Dansted and Slinko (2006). To generate an election with  $n$  voters who express preferences over  $m$  candidates, we proceed as follows. First, we form an urn that contains a single copy of every possible preference order (i.e., altogether  $m!$  votes). Then, to generate a vote, we draw a single preference order from the urn, include its copy in the election, and return it to the urn, together with  $\alpha m!$  of its copies. We repeat this process  $n$  times.

For  $\alpha = 0$  the urn model is equivalent to IC, whereas for  $\alpha = 1$  the probability that the second vote is identical to the first one is  $\frac{1}{2}$ . Generally, the larger is the parameter  $\alpha$ , the fewer clusters of identical votes, but each with more votes, are included in the generated elections (Faliszewski et al. (2023) give an upper bound on the expected number of clusters depending on  $\alpha$ ).

**Euclidean Models.** In the Euclidean models we assume that each candidate and each voter is represented as a point in some Euclidean space, and the voters prefer those candidates whose points are closer to theirs. Formally, if  $v$  is a voter,  $a, b$  are candidates, and the point of  $v$  is closer to that of  $a$  than to that of  $b$ , then  $v$  prefers  $a$  to  $b$  (we disregard the possibility of ties as, due to our way of generating the candidate and voter points, they occur with negligible probability<sup>2</sup>).

We consider two main ways of generating the points of the candidates and voters: Either we draw them uniformly at random from some  $d$ -dimensional hypercube, or from some  $d$ -dimensional hypersphere. Regarding the hypercube models, we consider the Interval model (points generated from a unit interval), the Square model (points generated from a square), the Cube model (points generated from a 3D cube), and 5D- and 10D Cube models (points generated from 5D and 10D cubes, respectively). Regarding the hypersphere models, we consider the Circle model (with the points generated from a circle in the 2D space) and the Sphere model (with the points generated from a 3D sphere).

**Single-Peaked Elections.** Let  $E = (C, V)$  be an election, where  $C = \{c_1, \dots, c_m\}$  and  $V = (v_1, \dots, v_n)$ . Further, let  $\triangleleft$  be strict linear order over  $C$ , referred to as the societal axis. We say that  $E$  is *single-peaked with respect to  $\triangleleft$*  if for every vote  $v_i$  and every  $t \in [m]$  the top  $t$  candidates in  $v_i$ 's preference order form an interval with respect to  $\triangleleft$ ;  $E$  is *single-peaked* if there is a societal axis with respect to which it is single-peaked. The notion of being *single-peaked on a circle (SPOC)* is defined analogously, except that for each voter  $v_i$  and each  $t \in [m]$  the top  $t$  candidates according to  $v_i$  either form an interval with respect to the societal axis or a complement of an interval. Single-peakedness was introduced by Black (1958) whereas single-peakedness on a circle was studied by Peters and Lackner (2020).

Intuitively, single-peaked elections capture settings where there is some objective, single-dimensional criterion (such as the political left-right spectrum, or a spectrum of possible temperatures in the room) with respect to which the candidates can be ordered, each voter has a favorite option, and the further a candidate is from this favorite one, the lower it is ranked by the respective voter. SPOC elections, on the other hand, capture such settings as voting on a time for a conference call when different participants are in different time zones.

We consider two models of generating single-peaked elections (in each model we draw the societal axis  $\triangleleft$  uniformly at random and then generate the votes one-by-one, independently):

1. In the Conitzer model (Conitzer 2009), denoted SP (Con), the process of generating a vote is as follows. First, we choose the top candidate uniformly at random. Then we perform  $m - 1$  steps where in each step we extend the vote with the next-best candidate, either located directly to the left (with respect to the societal axis) of

<sup>2</sup>Mathematically, the probability of a tie is zero, but due to finite nature of computation on real-life computers, it is slightly larger.

those already ranked, or directly to the right (the choice is made with probability  $1/2$ , unless there are no more candidates on one side, in which case the candidate from the other side is selected deterministically).

2. In the Walsh model (Walsh 2015), denoted SP (Wal), each single-peaked vote is generated with equal probability, uniformly at random.

For the case of SPOC elections, we generate the votes uniformly at random (indeed, in this case the naturally adapted variant of the Conitzer model coincides with that of Walsh).

**Group-Separable Elections.** Group-separable elections were introduced by Inada (Inada 1964, 1969), but in our discussion we will use the tree-based definition presented by Karpov (2019). Let  $C = \{c_1, \dots, c_m\}$  be a set of candidates and let  $\mathcal{T}$  be rooted, ordered tree with  $m$  leaves, where each leaf is labeled with a distinct candidate. For simplicity, we say that each internal node of  $\mathcal{T}$  orders its children from left to right. A *frontier* of  $\mathcal{T}$  is the preference order over  $C$  that ranks the candidates in the order in which we would visit them if we traversed  $\mathcal{T}$  using DFS, starting from the root and visiting each node's children in the order from left to right (intuitively, if we drew such a tree on paper, then we would obtain the frontier by reading the candidates in the leaves from left to right). A vote  $v$  is compatible with tree  $\mathcal{T}$  if it can be obtained as its frontier by reversing the order in which (some of) the internal nodes list their children. An election  $E = (C, V)$  is *group-separable* if there exists a rooted, ordered tree  $\mathcal{T}$ , where each leaf is labeled with a unique member of  $C$ , such that each vote in  $V$  is compatible with  $\mathcal{T}$ .

We are interested in two subclasses of group-separable elections:

1. We say that an election is *balanced group-separable*, denoted GS (bal), if it is group-separable with respect to some complete binary tree (i.e., a binary tree where all levels, except possibly for the last one, are filled completely).
2. We say that an election is *caterpillar group-separable*, denoted GS (cat), if it is group-separable with respect to some caterpillar binary tree (i.e., a binary tree where each node either is a leaf or one of its children is a leaf).

To generate a balanced (caterpillar) group-separable election, we start with an arbitrary balanced (caterpillar) tree that has its leaves labeled with the candidates that we are interested in and we generate votes one-by-one as follows: For each node of the tree, we reverse the order of its children with probability  $1/2$  and then we add the frontier of the tree to the election.

## B.2 Synthetic Datasets

We give the numbers of elections generated according to particular statistical cultures and included in the basic dataset in Table 1 (this dataset also includes special elections ID and AN, an approximate variant of UN, several artificial elections connecting these three, and the fourth special election, ST). The size-oriented and truncation-oriented datasets

Table 1: Numbers of elections generated according to our statistical cultures in the basic dataset. For the normalized Mallows elections, we choose norm- $\phi$  uniformly at random from interval  $[0, 1]$ . For the urn model, we choose the  $\alpha$  parameter according to the Gamma distribution with the shape parameter set to 0.8 and the scale parameter set to 1 (both parameterizations are in sync with previous datasets used in the maps of elections).

Statistical Culture	Number of Elections
Impartial Culture	16
Normalized Mallows	48
Urn	48
Interval	16
Square	16
Cube	16
5D Cube	8
10D Cube	8
Circle	16
Sphere	16
SP (Con)	16
SP (Wal)	16
SPOC	16
GS (Bal)	16
GS (Cat)	16

are readily obtained from the basic one, because for each statistical culture the number of elections generated according to it is divisible by 4 (hence, the process of generating these datasets, described in Section 4.1, is well-defined). Our basic dataset is nearly identical to the one used by Faliszewski et al. (2023). The difference is that we additionally include group-separable and SPOC elections, whereas they also included several real-life elections from Preflib (Mattei and Walsh 2013).

Regarding the comprehensive dataset, for most statistical cultures we can also proceed as described in Section 4.1 because the number of elections generated according to them is divisible by 16. The only exception regards 5D and 10D Cube elections, of which we have 8. For each of these cultures, we have 2 elections with either 8 or 16 candidates and either 96 or 192 voters. Among each pair of elections with the same size, one is left complete and one is truncated either according to the top- $k$  method or according to the random cut method (so, in particular, two of the 5D Cube elections are top- $k$  truncated, two are random-cut truncated, and four are left intact).

### C Swap Failure

In this section, we provide examples of swap distance failures (see also Section I for a proof of Theorem 3.3). We consider a smaller variant of the size-oriented dataset, obtained just like the original one, except that:

1. For each statistical culture, we generate only half the

Table 2: Axioms satisfied by the considered distance metrics.

metric	$\hat{d}_{\text{swap}}^{\text{del}}$	$\hat{d}_{\text{swap}}^{\text{tr}}$	$\hat{d}_{\text{pos}}$	$\hat{d}_{\text{dap}}$
triangle inequality	✗	✓	✓	✓
swap extension	✓	✓	✗	✗
pos. extension	✗	✗	✓	✗
ID-consistency	✓	✗	✗	✓
AN-consistency	✓	✗	✗	✓
UN-consistency	✗	✗	✓	✗

number of elections as in the size-based dataset, each of them with 96 voters.

2. Instead of considering elections with 8 and 16 candidates, we consider elections with 4 and 8 of them.

We refer to it as the size-based/mini dataset.

In Figure 8a we present a map of the size-based/mini dataset obtained using the truncation-based isomorphic swap distance. Secondly, in Figure 8b we present a map obtained using  $\hat{d}_{\text{swap}}^{\text{del}}$ , and in Figure 8c we present the same map but colored by the number of the triangle inequality violations (i.e., for each point we calculated how many triangles including that point violate the triangle inequality).

### D Satisfaction of Consistency Axioms

In Table 2, we present the satisfaction of axioms defined in Section 3, by two swap extensions,  $\hat{d}_{\text{swap}}^{\text{del}}$  and  $\hat{d}_{\text{swap}}^{\text{tr}}$  and positionwise distance,  $\hat{d}_{\text{pos}}$ , defined in Section 3.1 as well as DAP distance,  $\hat{d}_{\text{dap}}$ , defined in Section 3.2. Note the impossibility result of Theorem 3.1.

### E Varying Election Sizes for DAP

For the case of DAP, we have extended the first experiment from Section 4.3 to regard elections with up to 100 candidates (specifically, we have also included numbers of candidates in the set  $\{25, 30, 35, 40, 45, 50, 75, 100\}$ ). We show

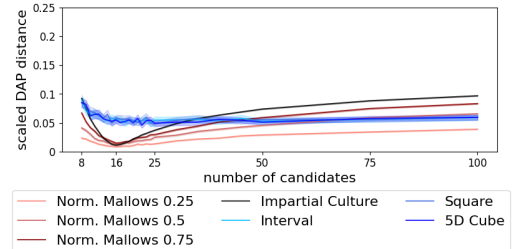


Figure 6: Average DAP distance from size-16 elections to different-sized, complete elections from the same culture as a fraction of a max. distance in our dataset.

the resulting plot in Figure 6. We see that as the number of candidates increases, the plots flatten out; e.g., for Euclidean elections at a bit over 6% and for IC at a bit over 10%.

## F Truncation Types Analysis

In this section, we give more in-depth analysis of the effect of different truncation types on positionwise and DAP distances.

Figure 7 presents average positionwise and DAP distances between a complete election and its different top-truncated variants. The plots were obtained in the second experiment from Section 4.3.

For positionwise distance (top row of Figure 7), the most affected by truncations are the cultures with the strongest structure (i.e., Mallows with a small parameter  $\text{norm-}\phi$  and interval elections) and the effect decreases when the elections become more chaotic. In particular, impartial culture is almost not affected at all by any of our truncation methods. The reason lies in the way positionwise distance handles the truncated votes: in frequency matrices, the values for unreported candidates are spread across several last positions. Hence, a frequency matrix of a heavily truncated election, becomes similar to the frequency matrix of a uniformity election.

Top- $k$  truncations (top left picture) and random cut truncations (top center picture) seem to have similar effect on positionwise distance. In both, the average distance is gradually increasing for all of the cultures (except impartial culture) as we truncate the election more and more.

On the other hand, for random drop truncations (top right picture), the distances quickly become large for the most structured cultures. In particular, when the votes have at most 8 reported candidates on average, for Mallows elections with  $\text{norm-}\phi = 0.25$ , the average distance is larger than the half of the diameter. This suggests that random drop truncation brings much more chaos into elections than the other two truncation methods. Indeed, under top- $k$  and random cut truncations the candidates in a few top positions of a vote will rarely end up in the truncated part. However, under random drop truncation there is a significant probability that we move a top candidate to a truncated part and another candidate becomes a top one.

For the DAP distance (bottom row of Figure 7), the question of which cultures are the most affected by truncation is no longer simple and consistent across the truncation types. For top- $k$  truncation (bottom left picture), for all cultures, the average distance is gradually increasing as we increase the range of truncation. Interestingly, the cultures most affected by top- $k$  truncation under DAP distance are exactly those that were least affected under positionwise distance (i.e., impartial culture and Mallows with  $\text{norm-}\phi = 0.75$ ). This is due to different treatment of truncations by DAP and positionwise distance (see Section 3.3). In heavily truncated elections voters agree that many pairs of candidates are equal, hence such elections are considered to be similar to identity. Thus, the most chaotic cultures are far away from such elections under DAP distance.

For random drop truncation (bottom right picture), we see a very interesting pattern for several cultures: the distance

quickly grows as the average number of reported candidates increases, but then it drops (and possibly increases again at the end). As discussed before, random drop truncation brings a lot of chaos into elections as candidates can move downward (when they land in the truncated part) or upward (when we drop candidates before them) in the votes. This explains a quick increase in the distance for highly structured cultures, such as Mallows with  $\text{norm-}\phi = 0.25$  or interval elections, where random drop truncation can destroy the structure. However, as votes become heavily truncated they start to become similar to each other in the sense that a lot of candidates are jointly seen as equally bad. Thus, such elections become similar to identity, which explains the movements of cultures in the right hand side of the plot.

Finally, for random cut truncation (bottom center picture) the plots look rather similar to that for top- $k$  truncation. The main differences are a bit larger average distances altogether and that the plot for Mallows with  $\text{norm-}\phi = 0.25$  resembles a bit its plot for random drop truncation but with a smaller amplitude. The similarity can be explained by the fact that random cut truncation is in some sense similar to top- $k$  truncation (the top part of each vote is exactly the same as in the original, complete election). The differences come from the fact that random cut truncation brings a bit more chaos than top- $k$  truncation since the votes can be cut in different points.

## G Extended Maps of Elections

Here we extend Section 4.2 and show maps of elections for the size-oriented, comprehensive and random drop datasets under both positionwise and DAP distances (see Figure 9). The random drop dataset was obtained by taking the basic one and applying random drop truncation to half of the elections from each statistical culture (so that, in expectation, each voter ranks half of the candidates).

For the size-oriented and comprehensive datasets, both DAP and positionwise maps look similar to the maps in Figure 2b and Figure 2a, respectively. Their shapes are preserved and truncated elections again cluster around UN and impartial culture under positionwise and around high dimensional Euclideans under DAP. Maps drawn from the random drop dataset show a similar overarching shape, but there the effect of truncation is much more prominent. Under both distances, the truncated elections form a dense cluster. This means that all such elections are much more similar in structure to each other than to complete elections from their respective cultures. This agrees with our observations from Figure 7, where for the average of half of the candidates reported (which is exactly the case for the random drop truncated elections in our dataset) for many cultures a complete election is on average far away from its random drop truncated version (e.g., for Mallows with  $\text{norm-}\phi = 0.25$ , it is around half of the diameter for both distances).

## H Extended Discussion of the Map of Preflib

In this section we provide a number of missing details and additional analyses regarding the map of Preflib—as well as

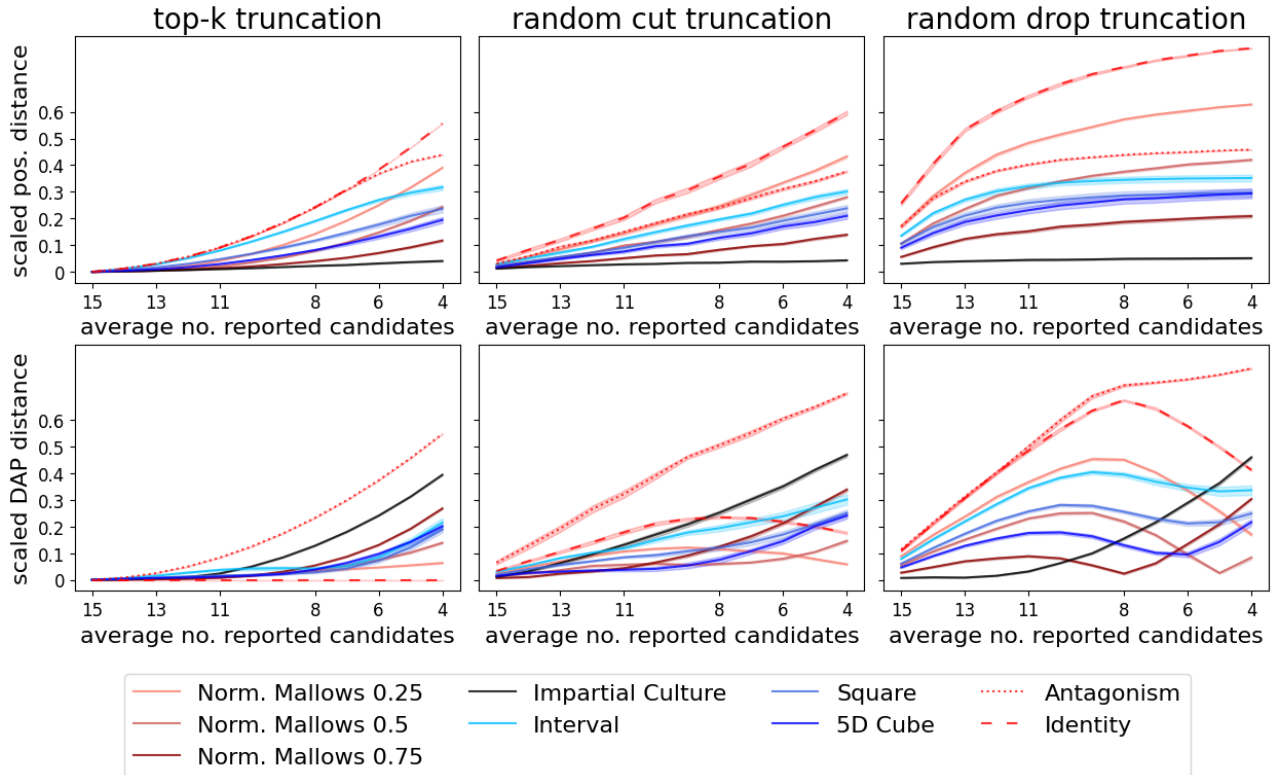


Figure 7: Average positionwise (top row) or DAP (bottom row) distances from a complete election to its top- $k$  (left column), random cut (center column), or random drop (right column) truncations as a fraction of a maximal distance in our dataset. Each datapoint is an average of 25 samples, the shaded area corresponds to the 95% confidence interval.

its several colorings—and the observations we make. First, we describe the contents of these map(s).

### H.1 Preflib Dataset Composition

We show several maps of Preflib. One in Figure 4, where all the Preflib election are represented as black dots for clarity, one in Figure 10, where for each Preflib election we indicate which exact Preflib dataset it comes from, several of them in Figure 11 colored by election type, and one in Figure 13, where we present a smaller fragment of Preflib (which we consider for the sake of the positionwise distance, see Section H.4). Next we describe the details of the Preflib dataset.

To construct the set of Preflib elections to include in our maps, we considered every dataset on Preflib with an *Election* tag and *.soc* or *.soi* file format (Preflib includes also other kinds of preference data, like matching data, and other preference formats, like cardinal or categorical preferences, that were not within the scope of this paper). We note that datasets vary greatly in the number of datafiles they contain (e.g., there is one file in the “T-Shirt” dataset, but 362 files in the “Spotify Daily Chart” dataset). To avoid overrepresentation of elections from datasets with numerous files in the map, from every dataset with more than 10 files, we have randomly chosen 10 files to include in the map.

We have also omitted some of the datasets introduced to Preflib by Boehmer and Schaar (2023). The nature of many

of these elections is very specific, as they report the given ranking evolving over time (e.g., in the “Spotify Countries Chart” dataset each file corresponds to a given country and a month and each vote represents the ranking of the 200 most listened songs on Spotify in this country on a particular day of this month, or in the “Formula 1 Races” dataset each file corresponds to a given Formula 1 race and each vote represents the ranking of drivers by the time in which they finished a particular lap).

Finally, to show which Preflib elections correspond to which statistical cultures, we added all cultures from the standard dataset and generated elections from these with 20 candidates and 1000 voters (number of candidates was higher here than in the standard dataset to adapt to Preflib elections, which on average tend to have a higher number of candidates). On our maps, we show these elections as much larger, pale discs, so that the Preflib elections are visible on top of them (depending on the particular maps, we either used the same—but more pale—colors as in the maps of synthetic elections, or we collapsed some of the colors into one; e.g., using the same pale blue for all Euclidean elections with points generated uniformly at random from hypercubes of various dimensions). In some of the maps, such as those in Figure 10 and Figure 11, we only kept synthetic elections generated using Mallows, urn, and Euclidean models (with points generated from hypercubes). For orientation

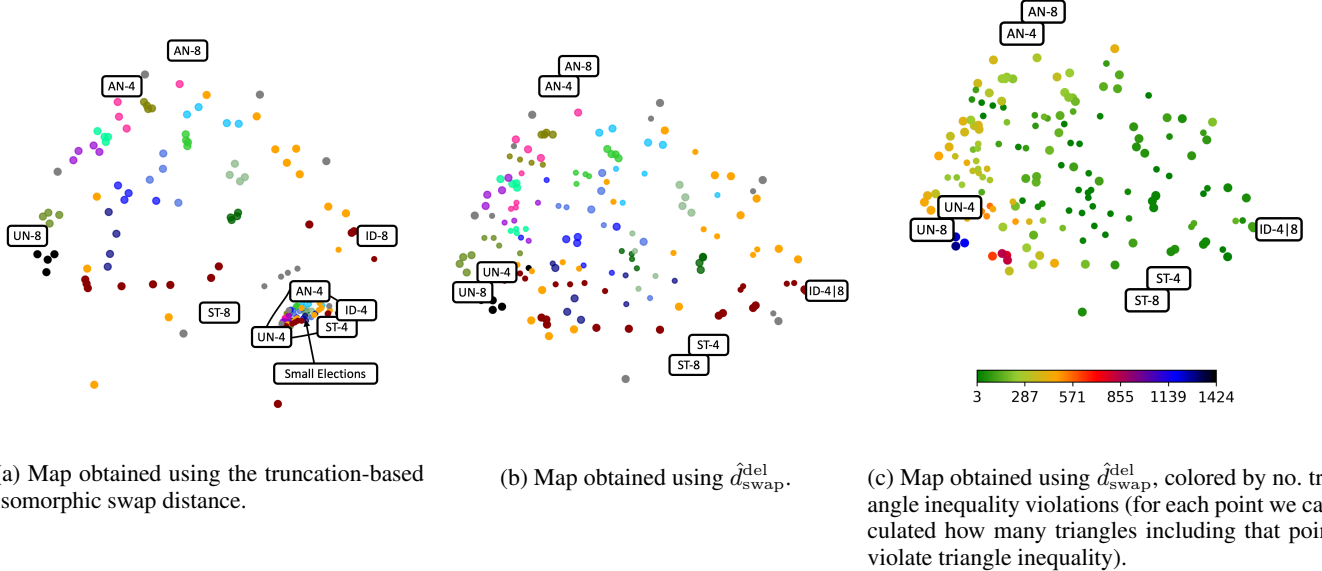


Figure 8: Maps showing various failures of the isomorphic swap distance extensions on the size-based/mini dataset.

purposes, we have added ID, AN, and an approximation of UN elections as well as elections forming paths between these three, each with 16 candidates and 500 voters.

Table 3 at the end of the appendix presents the exact composition of our Preflib dataset (excluding the artificial elections added for orientation and the synthetic ones). For each election, we report the corresponding Preflib file, the marker we use to denote its position on the maps in Figures 10, 11 and 13, the number of candidates, the number of votes, the number of unique votes, and the values of Diversity, Agreement, and Polarization indices, as well as the name of the statistical culture (and its parameters) of the synthetic election closest to it (in terms of DAP) in the dataset.

## H.2 Types of Elections

Following the information provided on Preflib, as well as the approach of Boehmer et al. (Boehmer et al. 2021, 2022a), we have classified the Preflib elections into five types (elections of each type are presented on the maps using their specific markers):

**Political elections (marked with squares).** By political elections, we mean elections where people cast votes over other people, to select someone—or a group of individuals—for some sort of a leadership position. These elections include, e.g., elections for the city council of Glasgow, elections in several districts in Ireland for their general elections, but also a number of elections from professional organizations, including those collected by Electoral Reform Society, elections for the president of the American Psychological Association, APA, or leadership elections held by the Debian project.

**Surveys (marked with dots).** Survey elections represent situations where people were asked to express their pref-

erences over a number of items. This includes, e.g., the classic Sushi dataset (Kamishima 2003), where people ranked sushi types, or surveys over breakfast items, opinions on movies, students’ preferences over university courses (AGH and Cujae) or various aspects of education (Cujae).

**Indicator (marked with diamonds).** Indicator elections rank various objects based on more-or-less objective criteria. This includes, e.g., rankings of universities according to different benchmarks, rankings of countries, or cities according to various quality-of-life measures.

**Mechanical Turk (marked with crosses).** These elections include rankings collected using Mechanical Turk by Andrew Mao. The tasks involved solving simple puzzles.

**Sports (marked with triangles).** Sports elections represent results of various competitions. For example, in the Formula 1 dataset each election represents a single season and each vote represents a single race. Sports elections also represent data on cycling races, skiing, and skating.

In Figure 11 we show maps of Preflib where only elections of a given type are highlighted, whereas all the other ones—including those generated synthetically and represented as large discs—are very pale. These maps lead to some interesting conclusions. Foremost, political (Figure 11b) and survey elections (Figure 11c) seem to be occupying roughly the same area of the map. One could point out to some minor differences (e.g., the political APA elections take an area that is not well-represented by the surveys elections, and the surveys WebSearch dataset takes an area that political elections do not often take) but, overall, these do not seem very relevant. Thus in experiments the two types of elections might be treated similarly (however, one should explore reasons for their similarity on our map in more de-

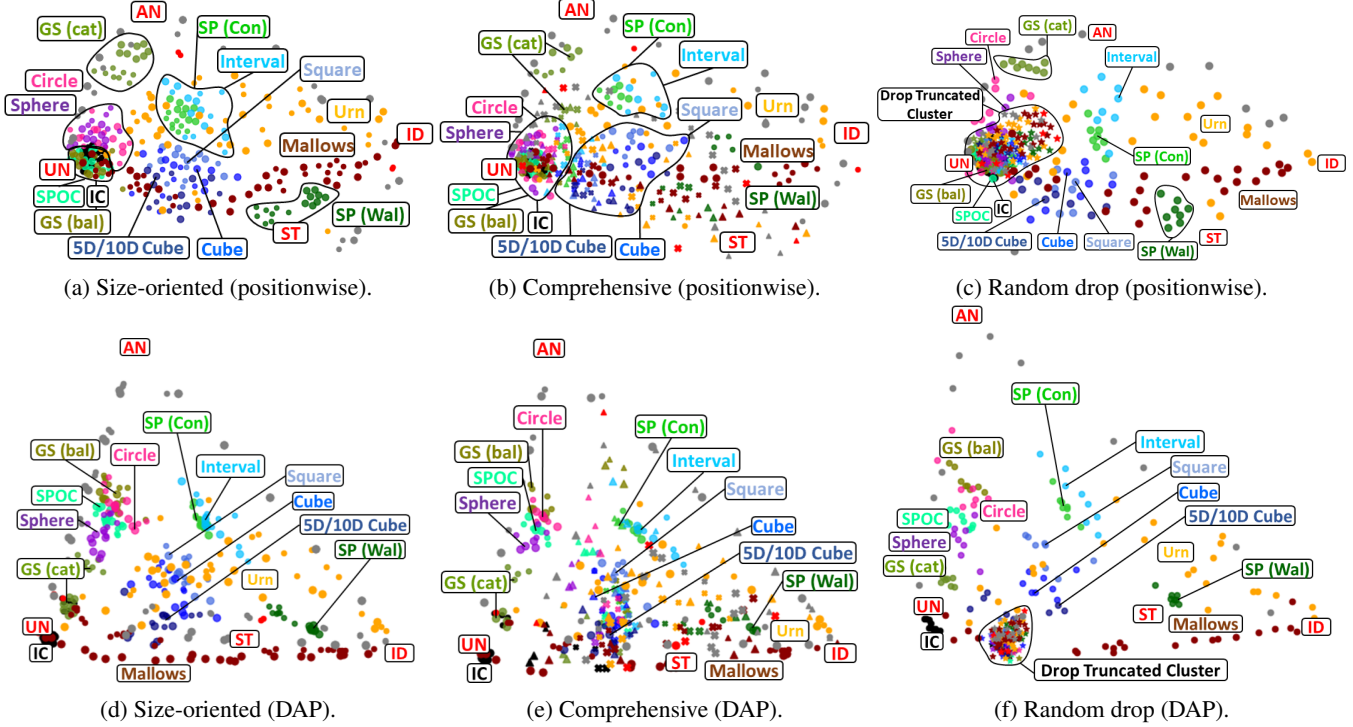


Figure 9: Maps of elections created using the positionwise (top), and DAP (bottom) distances, for the size-oriented (left), comprehensive (center), and random drop (right) datasets. Top- $k$  truncated elections are marked with triangles, random-cut truncated ones with crosses, random drop ones with stars and complete ones with circles. Larger markers mean elections with 16 candidates, and smaller markers mean elections with 8 candidates. In the ST election each voter ranks the same half of the candidates on top, but otherwise the votes are chosen uniformly at random.

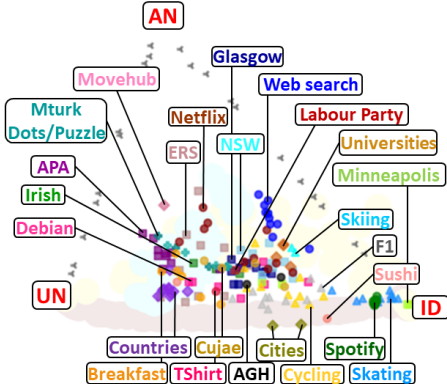


Figure 10: Map of Preflib, where colors and markers indicate the specific Preflib datasets from which each given election comes from. Large pale discs show synthetic elections generated using Mallows (pale brown), urn (pale yellow) or Euclidean elections with points generated uniformly at random from hypercubes (pale blue).

tail). The indicator elections (Figure 11d) take very specific, but quite spread out positions on the map. Given how few datasets in this category we have, it is not clear if we can draw any substantial conclusions. Rather, it seems that this

type of election may not stand out so much from the previous two types (but it might also be possible that indicator elections tend to assume very specific positions and we would see this more strongly given more data). Mechanical Turk elections (Figure 11e) also assume very specific positions, but also this might be simply because we have very few elections of this type, collected in very specific way (see the Preflib website for a description).

The only type of elections that truly stands out are the sports ones (Figure 11f). Essentially all of them are closer to ID than to UN (and, indeed, sometimes very close to ID, as in the case of the Skating dataset). This is natural as, indeed, we expect the sportsmen to perform similarly in different competitions. However, of course, the figure skating competitions held over a single day have much stronger correlation (position on the map very close to ID) than Formula 1 seasons, held over the course of a year, where drivers' abilities and performances can vary from a race to a race (similarly for cycling, where some participants are better on the flat areas of the race, and some do better in the climbing parts).

### H.3 Parameters of Mallows and Urn Elections Close to Preflib

We have attempted to establish the ranges of the norm- $\phi$  and contagion parameters for the Mallows and urn models that best capture many of the Preflib elections (omitting

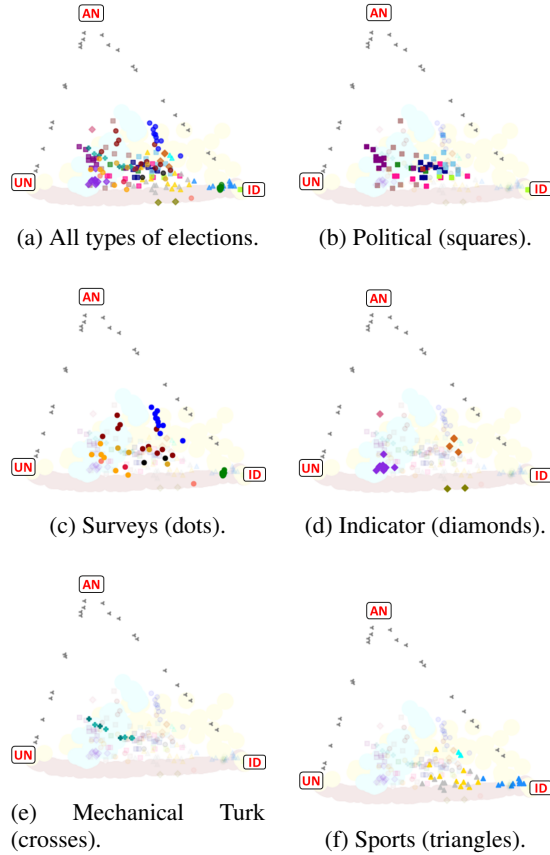


Figure 11: Map of Preflib with highlighted different types of elections. Large pale discs show synthetic elections generated using Mallows (pale brown), urn (pale yellow) or Euclidean elections with points generated uniformly at random from hypercubes (pale blue).

those very close to ID. In Figure 12a we show a map of Preflib where we indicate which elections we want to capture. Specifically, we seek norm- $\phi$  parameters of the Mallows elections whose  $x$ -positions on the map are between those shown by the left dashed line and the bottom-right one. Similarly, we seek contagion parameters of those urn elections whose  $x$ -coordinate is between the left and the top-right dashed lines. In Figures 12b and 12c we show relation between the  $x$ -positions on the map and the norm- $\phi$  and contagion parameters of the Mallows and urn elections, respectively. From these plots, we read off that the norm- $\phi$  parameters that we are after are in the range  $[0.2, 0.7]$ . For the case of the urn model, we can consider several options. If we choose the range  $[0.2, 0.5]$  of contagion parameters, then most of the generated elections will fall into the desired range of  $x$ -positions on the map, but we will miss some other urn elections in the range. If we consider range  $[0.2, 2]$ , then we get all urn elections from the desired area on the map, but also a number of others.

As a further validation of our recommendations, for each of the Preflib elections we found the closest synthetic elec-

tion in the dataset and recorded the statistical culture from which it comes from, as well as the parameter value for which it was generated (see the last column in Table 3). In most cases, these were either Mallows or urn elections, with parameters from the recommended ranges (but there were also cases where, e.g., an urn election with the contagion parameter around 3.62 was closest to a Preflib election<sup>3</sup>). However, hypercube elections (mostly for 5 and 10 dimensions) were also prominently represented, which justifies their use in experiments.

#### H.4 Positionwise Map of Preflib

Obtaining the map of Preflib elections similar to the one in Figure 4 but using positionwise distance is computationally difficult. This is due to large numbers of candidates in some of the elections, which leads to large sizes of frequency matrices. In this appendix, we present a positionwise map of a subset of elections from our Preflib dataset. Specifically, we removed all elections with more than 200 candidates (see Table 3 for an exact composition of our Preflib dataset). Figure 13a presents a positionwise distance map for this fragment of the dataset. For comparison, we have also included DAP distance map of the same fragment in Figure 13b.

We see that in positionwise map many elections are much closer to UN than in the DAP map. This can be explained by a different treatment of truncated elections by both distances (see Section 3.3). In particular, this affected many political elections, like elections from New South Wales (NSW) or Glasgow elections, which very often are heavily top-truncated (as voters report only a few top candidates).

## I Missing Proofs

In this appendix, we present the technical proofs that were omitted in the main part of the paper.

### I.1 Proof of Proposition 2.1

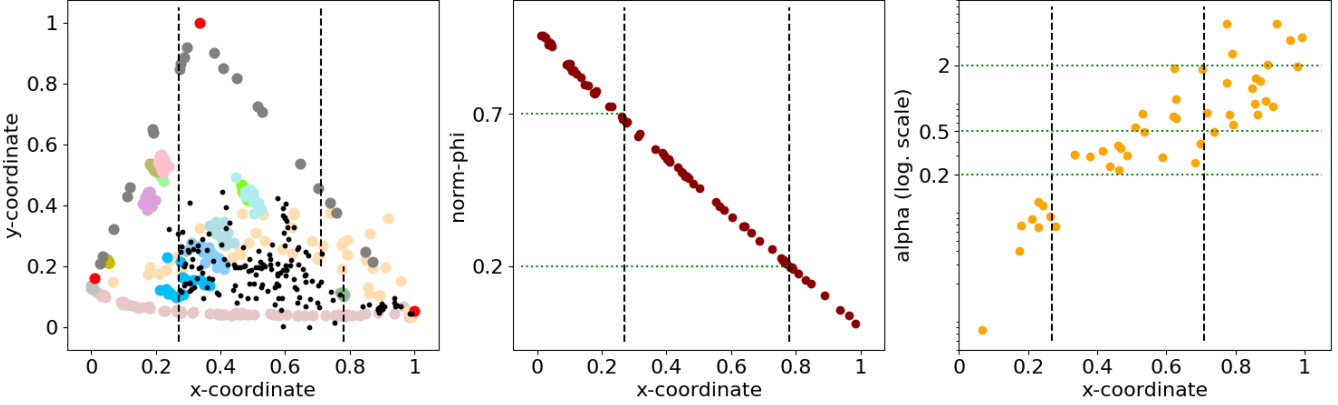
This proof is available in Section A.

### I.2 Proof of Proposition 3.1

*Proof.* First, let us show that there is no swap extension that satisfies ID-, AN- and UN-consistency. Assume, by contradiction, that there is such a swap extension  $\hat{d}^*$ . We know that  $d_{\text{swap}}(\text{AN}_{3,6}, \text{UN}_{3,6}) = 4/9 \neq 11/18 = d_{\text{swap}}(\text{AN}_{4,24}, \text{UN}_{4,24})$ . Consequently,  $\hat{d}^*(\text{AN}_{3,6}, \text{UN}_{3,6}) \neq \hat{d}^*(\text{AN}_{4,24}, \text{UN}_{4,24})$  as well. Since, by AN- and UN-consistency,  $\hat{d}^*(\text{AN}_{3,6}, \text{AN}_{4,24}) = \hat{d}^*(\text{UN}_{3,6}, \text{UN}_{4,24}) = 0$ , we get a violation of the triangle inequality.

Next, let us focus on positionwise extensions. To this end, let us establish the distances between UN and ID as well as UN and AN for equal and even number of candidates  $m$ . Denote uniformity vector  $\vec{u} = (1/m, 1/m, \dots, 1/m)$ , identity

<sup>3</sup>This was election 00018-00000003.soi from the Minneapolis dataset. However, this election is very particular as it captures a political elections with allowed write-ins. In effect, the election has nearly 500 candidates, including Mickey Mouse, that are mostly unranked.



(a) Map of Preflib elections. We attempt to capture the elections between dashed lines using the Mallows and urn models. Black dots represent Preflib elections, colorful ones represent synthetic ones (pale brown is for Mallows, pale yellow/orange for urn; other colors are as in Figure 4).

(b) Mallows norm- $\phi$  range. For each Mallows election (i.e., each dot), its  $x$  coordinate is the  $x$ -position on the map, and its  $y$ -coordinate is its norm- $\phi$  parameter.

(c) Urn parameter range. For each Urn election (i.e., each dot), its  $x$  coordinate is the  $x$ -position on the map, and its  $y$ -coordinate is its contagion parameter.

Figure 12: Ranges of norm- $\phi$  for the Mallows model and contagion parameters for the urn model that seem to capture Preflib elections well.

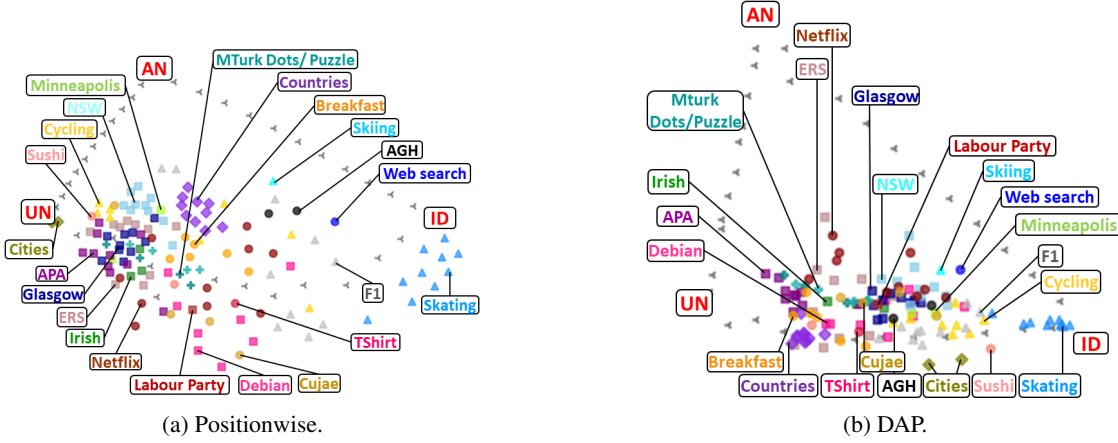


Figure 13: Maps of Preflib fragment.

vectors  $\vec{e}_i \in \mathbb{R}^m$  with 1 at  $i$ th position and zero otherwise, and antagonism vectors  $\vec{a}_i \in \mathbb{R}^m$  with  $1/2$  at  $i$ th and  $m - i$ th positions and zero otherwise. It is easy to verify that for  $m = 2k$ , it holds that

$$W(\vec{u}, \vec{e}_i) = \frac{1}{2m^2} ((i-1)^2 + (m-i)^2 + m-1) \quad \text{and}$$

$$W(\vec{u}, \vec{a}_i) = \frac{1}{4k^2} \left( (i-1)^2 + (k-i)^2 + \frac{(i-1)^2 + (k-i)^2}{k-1} \right).$$

By summing the above equations for all  $i \in [m]$ , we obtain

that

$$d_{\text{pos}}(\text{UN}_m, \text{ID}_m) = \frac{1}{3} - \frac{1}{3m^2} \quad \text{and}$$

$$d_{\text{pos}}(\text{UN}_m, \text{AN}_m) = \frac{1}{6} - \frac{1}{6m}.$$

Now, assume that there exists a positionwise extension  $\hat{d}^*$  that satisfies ID-, AN, and UN-consistency. This means that both  $\hat{d}^*(\text{UN}_{m,n}, \text{ID}_{m,n})$  and  $\hat{d}^*(\text{UN}_{m,n}, \text{AN}_{m,n})$  have to be constant for different values of  $m$  and  $n$  (as  $\hat{d}^*$  must satisfy the triangle inequality in addition to the consistency properties). However, since we have shown that  $d_{\text{pos}}(\text{UN}_m, \text{ID}_m)/d_{\text{pos}}(\text{UN}_m, \text{AN}_m)$  is not constant for different values of  $m$ , this is not possible if  $\hat{d}^*$  is a posi-

tionwise extension.  $\square$

### I.3 Proof of Proposition 3.3

*Proof.* Let  $E = (C, V)$  be an election with three candidates,  $C = \{a, b, c\}$ , and six voters:

$$\begin{aligned} v_1: a > b > c, \quad v_3: b > c > a, \quad v_5: c > a > b, \\ v_2: a > b > c, \quad v_4: b > c > a, \quad v_6: c > a > b, \end{aligned}$$

and let  $ID_{3,6}$  be an identity election with six voters, each with preference order  $x > y > z$ . One can verify that  $\hat{d}_{\text{swap}}^{\text{del}}(E, ID_{3,6}) = 8/9$  (indeed, there are no candidates to delete, it takes 8 swaps to make all votes identical in  $E$ , and the normalizing factor is 9).

Next, let us consider election  $ID_{2,6}$ , where each of the six voters has preference order  $x > y$ . For each election  $E'$  obtained from  $E$  by deleting a single candidate, we have  $\hat{d}_{\text{swap}}^{\text{del}}(E', ID_{2,6}) = 2/3$  (it suffices to make two swaps in  $E'$  to ensure that all the votes are identical, and the normalizing factor is 3). We also see that  $\hat{d}_{\text{swap}}^{\text{del}}(ID_{2,6}, ID_{3,6}) = 0$ . Then,  $\hat{d}_{\text{swap}}^{\text{del}}(E, ID_{3,6}) > \hat{d}_{\text{swap}}^{\text{del}}(E, ID_{2,6}) + \hat{d}_{\text{swap}}^{\text{del}}(ID_{2,6}, ID_{3,6})$  and, so,  $\hat{d}_{\text{swap}}^{\text{del}}$  fails the triangle inequality.  $\square$

### I.4 Proof of Theorem 3.4

We first show that the Wasserstein distance between matrices is invariant to stretching these matrices.

**Lemma I.1.** *Let  $X = [\vec{x}_1, \dots, \vec{x}_m]$  and  $Y = [\vec{y}_1, \dots, \vec{y}_m]$  be two frequency matrices, and let  $t$  be a nonnegative integer. Then  $d_W(X, Y) = d_W(\text{str}_{mt}(X), \text{str}_{mt}(Y))$ .*

*Proof.* To prove this result, we need to recall the way of computing the Wasserstein distance between two matrices, provided by Szufa et al. (2020). Let  $A = [\vec{a}_1, \dots, \vec{a}_k]$  and  $B = [\vec{b}_1, \dots, \vec{b}_k]$  be two matrices, whose column vectors have nonnegative entries that sum up to 1 (for each vector). To compute  $d_W(A, B)$ , we form flow network  $N(A, B)$  that contains source  $s$ , nodes  $a_1, \dots, a_k$ , nodes  $b_1, \dots, b_k$ , and sink  $t$  (by a slight abuse of notation, we use the same names for both the nodes of the network and the vectors in respective matrices, except that for the nodes we omit the arrows on top of them). For each  $i \in [k]$ , there is an arc from  $s$  to  $a_i$  and an arc from  $b_i$  to  $t$  (each of these arcs has capacity 1 and cost 0). Further, for each  $i, j \in [k]$ , there is an arc from  $a_i$  to  $b_j$  with capacity 1 and cost  $\frac{1}{k}W(\vec{a}_i, \vec{b}_j)$ . One can verify that in this network the min-cost flow of value  $k$  from  $s$  to  $t$  has cost equal to  $d_W(A, B)$ .

Next, consider networks  $N_m = N(X, Y)$  and  $M_{mt} = N(\text{str}_{mt}(X), \text{str}_{mt}(Y))$ . For each  $i \in [m]$  and  $p \in [t]$ , we write  $\vec{x}_i^{(p)}$  to refer to the  $p$ -th copy of vector  $\vec{x}_i$  that  $\text{str}_{mt}(X)$  contains. The meaning of  $\vec{y}_i^{(p)}$  is analogous. Let  $f_m$  be a min-cost flow of value  $m$  from  $s$  to  $t$  in  $N_m$  and, analogously, let  $f_{mt}$  be a min-cost flow of value  $mt$  from  $s$  to  $t$  in  $N_{mt}$ . We claim that the costs of  $f_m$  and  $f_{mt}$  are equal (and, hence,  $d_W(X, Y) = d_W(\text{str}_{mt}(X), \text{str}_{mt}(Y))$ ). First, we observe that the cost of  $f_{mt}$  is greater or equal to that of  $f_m$ . To see why this is the case, consider flow  $g$  in  $N_m$  defined as follows:

1. For each  $i \in [m]$  there is flow of value 1 from  $s$  to  $x_i$ , and from  $y_i$  to  $t$ .
2. For each  $i, j \in [m]$ , there is flow of value  $\sum_{p \in [t], q \in [t]} \frac{1}{t} f_{mt}(x_i^{(p)}, y_j^{(q)})$  from  $x_i$  to  $y_j$ .

Note that since  $f_{mt}$  is a correct flow, so is  $g$ , and indeed  $g$  moves  $m$  units of flow from  $s$  to  $t$ . Further, the cost of  $g$  in  $N_m$  is the same as the cost of  $f_{mt}$  in  $N_{mt}$ . Since  $f_m$  is a min-cost flow of value  $m$ , its cost cannot be larger than that of  $g$ . An analogous argument shows that the cost of  $f_m$  is greater or equal to that of  $f_{mt}$ . Hence the two flows have equal costs, which proves the lemma.  $\square$

Next, we show that  $\hat{d}_{\text{pos}}$  is a pseudodistance.

**Proposition I.2.** *Function  $\hat{d}_{\text{pos}}$  is a pseudodistance.*

*Proof.* It is immediate to see that for each two elections  $E$  and  $F$ , we have  $\hat{d}_{\text{pos}}(E, E) = 0$ ,  $\hat{d}_{\text{pos}}(E, F) \geq 0$ , and  $\hat{d}_{\text{pos}}(E, F) = \hat{d}_{\text{pos}}(F, E)$ . It remains to argue that we also have the triangle inequality.

Let  $A, B$ , and  $C$  be three elections with, respectively,  $p, q$ , and  $r$  candidates. Further, let  $P, Q$ , and  $R$  be their frequency matrices. Our goal is to show that:

$$\hat{d}_{\text{pos}}(A, B) + \hat{d}_{\text{pos}}(B, C) \geq \hat{d}_{\text{pos}}(A, C).$$

By the definition of  $\hat{d}_{\text{pos}}$  and Theorem I.1, this is equivalent to:

$$d_W(\text{str}_{pqr}(P), \text{str}_{pqr}(Q)) + d_W(\text{str}_{pqr}(Q), \text{str}_{pqr}(R)) \geq d_W(\text{str}_{pqr}(P), \text{str}_{pqr}(R))$$

Since  $d_W$  satisfies the triangle inequality (this has been shown by Szufa et al. (2020)), this inequality must hold.  $\square$

### I.5 Proof of Proposition 3.6

*Proof.* We begin by showing a useful fact about the uniformity elections with a large number of candidates. It turns out that in such elections every vote is in approximately half of a maximal swap distance to almost every other vote.

**Lemma I.3.** *For every  $\varepsilon, d > 0$ , there exists  $M \in \mathbb{N}$  such that for every  $m \geq M$ ,  $(C, V) = \text{UN}_{m, m!}$ , and  $u \in V$ , it holds that*

$$\left| \left\{ v \in V : \frac{\text{swap}(u, v)}{\binom{m}{2}} \notin \left( \frac{1}{2} - \varepsilon, \frac{1}{2} + \varepsilon \right) \right\} \right| \leq d \cdot m!.$$

*Proof.* Let us denote the left hand side of the inequality in the lemma statement by  $L_m$ . Fix  $m \in \mathbb{N}$ ,  $(C, V) = \text{UN}_{m, m!}$ , and  $u \in V$ . Consider drawing a random vote  $v$  from  $V$  and random variable  $x = \text{swap}(u, v)$ . This variable follows so called *Mahonian distribution* (Ben-Naim 2010) and it is known that its mean and variance are equal to

$$\mu = \frac{m(m-1)}{4} \quad \text{and} \quad \sigma^2 = \frac{m(m-1)(2m+5)}{72},$$

respectively. Then, from Chebyshev's inequality for the random variable  $x/\binom{m}{2}$ , for every  $\varepsilon > 0$ , it holds that

$$\mathbb{P} \left( \left| \frac{x}{\binom{m}{2}} - \frac{\mu}{\binom{m}{2}} \right| \geq \varepsilon \right) \leq \frac{\sigma^2}{\binom{m}{2}^2 \varepsilon^2} = \frac{O(m^{-1})}{\varepsilon^2}.$$

Since  $\mu/\binom{m}{2} = 1/2$ , we get that  $|x/\binom{m}{2} - \mu/\binom{m}{2}| \geq \varepsilon$  is equivalent to  $\text{swap}(u, v)/\binom{m}{2} \notin (1/2 - \varepsilon, 1/2 + \varepsilon)$ . Thus, we obtain  $L_m/m! \leq O(m^{-1})/\varepsilon^2$ . The fact that  $O(m^{-1})$  becomes arbitrarily small as  $m$  grows yields the thesis.  $\square$

In the remainder of the proof, let us show that for every  $\varepsilon > 0$ , there exists  $M \in \mathbb{N}$  such that for every  $m \geq M$ , it holds that  $\text{emk}_i(\text{UN}_{m,m!})/(m!\binom{m}{2}) \geq 1/2 - \varepsilon$ . Since for every  $m$  we have  $\text{emk}_i(\text{UN}_{m,m!}) \leq 1/2 \cdot m!\binom{m}{2}$  (this is the maximum Kemeny distance), this will imply the thesis.

Fix  $\varepsilon > 0$ . Let us take arbitrary  $m \in \mathbb{N}$  such that  $\text{emk}_i(\text{UN}_{m,m!})/(m!\binom{m}{2}) < 1/2 - \varepsilon$ . By definition, this means that there exist votes  $v_1, \dots, v_i \in V$  such that

$$\frac{1}{m!} \sum_{v \in V} \min_{j \in [i]} \frac{\text{swap}(v, v_j)}{\binom{m}{2}} < \frac{1}{2} - \varepsilon. \quad (3)$$

Let us denote the left hand side of the above inequality by  $L$ . Next, let us split the set of voters,  $V$ , into two disjoint sets,  $V^+ = \{v \in V : \min_{j \in [i]} \text{swap}(v, v_j)/\binom{m}{2} \geq 1/2 - \varepsilon/2\}$  and  $V^- = V \setminus V^+$ . Observe that

$$\begin{aligned} L &= \frac{1}{m!} \left( \sum_{v \in V^+} \min_{j \in [i]} \frac{\text{swap}(v, v_j)}{\binom{m}{2}} + \sum_{v \in V^-} \min_{j \in [i]} \frac{\text{swap}(v, v_j)}{\binom{m}{2}} \right) \\ &\geq \frac{|V^+|}{m!} \left( \frac{1}{2} - \frac{\varepsilon}{2} \right). \end{aligned}$$

Combining this with inequality (3) we get

$$|V^+| \leq m! \cdot \frac{\frac{1}{2} - \varepsilon}{\frac{1}{2} - \frac{\varepsilon}{2}}.$$

Hence, there exists  $\varepsilon' = \varepsilon/(1 - \varepsilon) > 0$  such that  $|V^+| \leq m! \cdot (1 - \varepsilon')$ . Thus,  $|V^-| > m! \cdot \varepsilon'$ , i.e.,

$$\left| \left\{ v \in V : \min_{j \in [i]} \frac{\text{swap}(u, v)}{\binom{m}{2}} < \frac{1}{2} - \frac{\varepsilon}{2} \right\} \right| > m! \cdot \varepsilon'.$$

Hence, there exists  $j \in [i]$  such that

$$\left| \left\{ v \in V : \frac{\text{swap}(u, v)}{\binom{m}{2}} < \frac{1}{2} - \frac{\varepsilon}{2} \right\} \right| > m! \cdot \frac{\varepsilon'}{i}.$$

By Lemma I.3, there exists  $M \in \mathbb{N}$  such that for every  $m \geq M$  the above inequality does not hold. Therefore, for each such  $m$ , it holds that  $\text{emk}_i(\text{UN}_{m,m!})/(m!\binom{m}{2}) \geq 1/2 - \varepsilon$ , which concludes the proof.  $\square$

Election Name	Marker	Preflib File	#Candidates	#Votes	Diversity	Agreement	Polarization	Closest Culture
Irish (1)	■	00001-00000001.soi	12	43942	0.42*	0.41	0.16*	Urn, $\alpha = 0.24$ (0.05)
Irish (2)	■	00001-00000002.soi	9	29988	0.46*	0.33	0.18*	Urn, $\alpha = 0.3$ (0.01)
Irish (3)	■	00001-00000003.soi	14	64081	0.37*	0.48	0.14*	Urn, $\alpha = 0.22$ (0.1)
Debian (1)	■	00002-00000001.soi	4	475	0.28	0.51	0.16	Urn, $\alpha = 0.29$ (0.03)
Debian (2)	■	00002-00000002.soi	5	488	0.35	0.47	0.16	Urn, $\alpha = 0.29$ (0.07)
Debian (3)	■	00002-00000003.soi	7	504	0.44	0.43	0.1	Cube (0.07)
Debian (4)	■	00002-00000004.soi	8	421	0.4	0.51	0.06	Mallows, $\text{norm-}\phi = 0.46$ (0.07)
Debian (5)	■	00002-00000005.soi	9	482	0.51	0.35	0.13	5-Cube (0.03)
Debian (6)	■	00002-00000006.soi	5	436	0.32	0.55	0.1	Urn, $\alpha = 0.69$ (0.1)
Debian (7)	■	00002-00000007.soi	4	403	0.2	0.67	0.09	Urn, $\alpha = 1.39$ (0.06)
Debian (8)	■	00002-00000008.soi	8	143	0.5	0.35	0.13	Cube (0.04)
Netflix (1)	●	00004-00000013.soc	3	617	0.2	0.48	0.25	Urn, $\alpha = 1.88$ (0.05)
Netflix (2)	●	00004-00000092.soc	3	1631	0.31	0.26	0.32	Square (0.07)
Netflix (3)	●	00004-00000111.soc	4	390	0.32	0.46	0.17	Urn, $\alpha = 0.49$ (0.09)
Netflix (4)	●	00004-00000123.soc	4	376	0.37	0.32	0.29	Square (0.02)
Netflix (5)	●	00004-00000147.soc	4	400	0.45	0.25	0.24	Cube (0.03)
Netflix (6)	●	00004-00000148.soc	4	485	0.29	0.49	0.18	Urn, $\alpha = 0.29$ (0.06)
Netflix (7)	●	00004-00000164.soc	4	512	0.35	0.32	0.3	Square (0.02)
Netflix (8)	●	00004-00000178.soc	4	366	0.22	0.61	0.12	Urn, $\alpha = 0.38$ (0.08)
Netflix (9)	●	00004-00000179.soc	4	454	0.25	0.56	0.16	Urn, $\alpha = 0.29$ (0.07)
Netflix (10)	●	00004-00000186.soc	4	417	0.27	0.54	0.14	Urn, $\alpha = 0.29$ (0.08)
Skating (1)	▲	00006-00000003.soc	14	9	0.04	0.92	0.03	Mallows, $\text{norm-}\phi = 0.06$ (0.04)
Skating (2)	▲	00006-00000008.soc	23	9	0.04	0.94	0.01	Mallows, $\text{norm-}\phi = 0.06$ (0.02)
Skating (3)	▲	00006-00000011.soc	20	9	0.07	0.9	0.02	Mallows, $\text{norm-}\phi = 0.1$ (0.03)
Skating (4)	▲	00006-00000018.soc	24	9	0.03	0.95	0.01	Mallows, $\text{norm-}\phi = 0.04$ (0.01)
Skating (5)	▲	00006-00000028.soc	24	9	0.13	0.85	0.04	Mallows, $\text{norm-}\phi = 0.14$ (0.03)
Skating (6)	▲	00006-00000029.soc	19	9	0.11	0.86	0.04	Mallows, $\text{norm-}\phi = 0.14$ (0.04)
Skating (7)	▲	00006-00000033.soc	23	9	0.06	0.9	0.03	Mallows, $\text{norm-}\phi = 0.1$ (0.05)
Skating (8)	▲	00006-00000036.soc	18	9	0.17	0.76	0.08	Single Peaked, Walsh (0.01)
Skating (9)	▲	00006-00000046.soc	30	7	0.04	0.93	0.02	Mallows, $\text{norm-}\phi = 0.06$ (0.02)
Skating (10)	▲	00006-00000048.soc	24	9	0.05	0.93	0.02	Mallows, $\text{norm-}\phi = 0.06$ (0.02)
ERS (1)	■	00007-00000013.soi	5	2785	0.5	0.3	0.16	Cube (0.04)
ERS (2)	■	00007-00000026.soi	5	148	0.41	0.32	0.23	Square (0.01)
ERS (3)	■	00007-00000029.soi	17	176	0.36	0.4	0.23	Urn, $\alpha = 0.37$ (0.03)
ERS (4)	■	00007-00000032.soi	13	575	0.51	0.39	0.09	5-Cube (0.04)
ERS (5)	■	00007-00000037.soi	10	460	0.6	0.28	0.09	10-Cube (0.03)
ERS (6)	■	00007-00000050.soi	10	195	0.32	0.49	0.16	Urn, $\alpha = 0.29$ (0.09)
ERS (7)	■	00007-00000063.soi	3	213	0.32	0.25	0.4	Interval (0.13)
ERS (8)	■	00007-00000065.soi	8	362	0.44	0.29	0.28	Square (0.03)
ERS (9)	■	00007-00000078.soi	20	365	0.55	0.36	0.07	5-Cube (0.05)
ERS (10)	■	00007-00000079.soi	14	661	0.45	0.47	0.08	Mallows, $\text{norm-}\phi = 0.49$ (0.08)
Glasgow (1)	■	00008-00000001.soi	9	6900	0.39	0.46	0.17	Urn, $\alpha = 0.37$ (0.08)
Glasgow (2)	■	00008-00000005.soi	10	11052	0.35	0.5	0.19	Urn, $\alpha = 0.29$ (0.1)
Glasgow (3)	■	00008-00000008.soi	10	10160	0.32	0.52	0.17	Urn, $\alpha = 0.29$ (0.08)
Glasgow (4)	■	00008-00000009.soi	11	9560	0.31	0.56	0.16	Urn, $\alpha = 0.29$ (0.09)
Glasgow (5)	■	00008-00000010.soi	9	8682	0.38	0.45	0.2	Urn, $\alpha = 0.37$ (0.06)
Glasgow (6)	■	00008-00000011.soi	10	8984	0.39	0.47	0.11	Urn, $\alpha = 0.22$ (0.12)
Glasgow (7)	■	00008-00000015.soi	9	8654	0.37	0.48	0.17	Urn, $\alpha = 0.22$ (0.09)
Glasgow (8)	■	00008-00000018.soi	9	9567	0.39	0.49	0.12	Mallows, $\text{norm-}\phi = 0.46$ (0.12)
Glasgow (9)	■	00008-00000019.soi	11	8803	0.32	0.55	0.16	Urn, $\alpha = 0.29$ (0.1)
Glasgow (10)	■	00008-00000021.soi	10	5410	0.29	0.57	0.14	Urn, $\alpha = 0.29$ (0.1)
AGH (1)	●	00009-00000001.soc	9	146	0.36	0.51	0.11	Mallows, $\text{norm-}\phi = 0.41$ (0.12)
AGH (2)	●	00009-00000002.soc	7	153	0.27	0.59	0.12	Urn, $\alpha = 0.38$ (0.12)
Skiing (1)	▲	00010-00000001.soi	351	4	0.18	0.59	0.18	Urn, $\alpha = 0.38$ (0.04)

Election Name	Marker	Preflib File	#Candidates	#Votes	Diversity	Agreement	Polarization	Closest Culture
Skiing (2)	▲	00010-00000002.soi	170	4	0.18	0.58	0.2	Urn, $\alpha = 0.38$ (0.06)
Web search (1)	●	00011-00000003.soc	103	5	0.15	0.64	0.2	Urn, $\alpha = 0.38$ (0.05)
Web search (2)	●	00011-00000006.soi	1449	4	0.17	0.5	0.26	Urn, $\alpha = 1.88$ (0.03)
Web search (3)	●	00011-00000008.soi	1572	4	0.18	0.45	0.34	Urn, $\alpha = 0.66$ (0.07)
Web search (4)	●	00011-00000010.soi	2096	4	0.2	0.5	0.23	Urn, $\alpha = 0.29$ (0.05)
Web search (5)	●	00011-00000012.soi	1210	4	0.16	0.46	0.36	Urn, $\alpha = 0.66$ (0.06)
Web search (6)	●	00011-00000038.soi	1754	4	0.18	0.46	0.3	Urn, $\alpha = 1.88$ (0.05)
Web search (7)	●	00011-00000049.soi	1845	4	0.18	0.43	0.38	Interval (0.08)
Web search (8)	●	00011-00000052.soi	2242	4	0.18	0.47	0.29	Urn, $\alpha = 1.88$ (0.04)
Web search (9)	●	00011-00000054.soi	2512	4	0.19	0.49	0.27	Urn, $\alpha = 1.88$ (0.03)
Web search (10)	●	00011-00000071.soi	2127	4	0.18	0.46	0.31	Urn, $\alpha = 1.88$ (0.06)
TShirt	●	00012-00000001.soc	11	30	0.46	0.43	0.09	Cube (0.09)
Sushi (1)	●	00014-00000001.soc	10	5000	0.54	0.32	0.14	5-Cube (0.02)
Sushi (2)	●	00014-00000002.soi	100	5000	0.26	0.81	0.02	Mallows, norm- $\phi = 0.23$ (0.05)
Minneapolis (1)	■	00018-00000001.soi	379	36655	0.01	0.99	0	Mallows, norm- $\phi = 0.01$ (0)
Minneapolis (2)	■	00018-00000002.soi	9	36655	0.33	0.56	0.12	Mallows, norm- $\phi = 0.39$ (0.12)
Minneapolis (3)	■	00018-00000003.soi	477	32086	0	0.99	0	Urn, $\alpha = 3.62$ (0.01)
Minneapolis (4)	■	00018-00000004.soi	7	32086	0.27	0.6	0.09	Urn, $\alpha = 0.38$ (0.12)
MTurk Dots (1)	✚	00024-00000001.soc	4	795	0.49	0.18	0.26	Cube (0.06)
MTurk Dots (2)	✚	00024-00000002.soc	4	794	0.46	0.25	0.22	Cube (0.03)
MTurk Dots (3)	✚	00024-00000003.soc	4	800	0.41	0.36	0.15	Cube (0.03)
MTurk Dots (4)	✚	00024-00000004.soc	4	794	0.37	0.42	0.15	Urn, $\alpha = 0.22$ (0.05)
MTurk Puzzle (1)	✚	00025-00000001.soc	4	793	0.48	0.22	0.23	Cube (0.03)
MTurk Puzzle (2)	✚	00025-00000002.soc	4	795	0.37	0.42	0.15	Urn, $\alpha = 0.22$ (0.05)
MTurk Puzzle (3)	✚	00025-00000003.soc	4	795	0.4	0.38	0.16	Urn, $\alpha = 0.24$ (0.03)
MTurk Puzzle (4)	✚	00025-00000004.soc	4	797	0.44	0.28	0.2	Cube (0.04)
APA (1)	■	00028-00000001.soi	5	18723	0.53	0.24	0.16	Cube (0.04)
APA (2)	■	00028-00000002.soi	5	17469	0.54	0.16	0.3	Urn, $\alpha = 0.31$ (0.09)
APA (3)	■	00028-00000003.soi	5	20239	0.51	0.25	0.21	Cube (0.04)
APA (4)	■	00028-00000004.soi	5	17911	0.53	0.22	0.21	Cube (0.04)
APA (5)	■	00028-00000006.soi	5	17956	0.41	0.41	0.16	Urn, $\alpha = 0.22$ (0.03)
APA (6)	■	00028-00000008.soi	5	14506	0.5	0.26	0.22	Cube (0.05)
APA (7)	■	00028-00000009.soi	5	16836	0.51	0.26	0.18	Cube (0.05)
APA (8)	■	00028-00000010.soi	5	13318	0.53	0.22	0.24	Cube (0.05)
APA (9)	■	00028-00000011.soi	5	18286	0.51	0.24	0.22	Cube (0.05)
APA (10)	■	00028-00000012.soi	5	15313	0.53	0.2	0.28	Cube (0.06)
Labour Party	■	00030-00000001.soi	5	266	0.36	0.45	0.14	Urn, $\alpha = 0.22$ (0.1)
Cujae (1)	●	00032-00000001.soi	6	32	0.39	0.41	0.16	Urn, $\alpha = 0.22$ (0.05)
Cujae (2)	●	00032-00000002.soc	6	15	0.31	0.5	0.17	Urn, $\alpha = 0.29$ (0.07)
Cujae (3)	●	00032-00000003.soi	6	47	0.43	0.36	0.19	Cube (0.03)
Cujae (4)	●	00032-00000005.soi	13	14	0.28	0.62	0.1	Mallows, norm- $\phi = 0.33$ (0.1)
Cities (1)	■	00034-00000001.soi	36	392	0.43	0.69	0.06	Mallows, norm- $\phi = 0.36$ (0.09)
Cities (2)	■	00034-00000002.soi	48	392	0.35	0.76	0.04	Mallows, norm- $\phi = 0.31$ (0.09)
Breakfast (1)	●	00035-00000002.soc	15	42	0.53	0.31	0.18	5-Cube (0.05)
Breakfast (2)	●	00035-00000003.soc	15	42	0.47	0.47	0.05	Mallows, norm- $\phi = 0.51$ (0.05)
Breakfast (3)	●	00035-00000004.soc	15	42	0.57	0.27	0.19	5-Cube (0.03)
Breakfast (4)	●	00035-00000005.soc	15	42	0.51	0.29	0.24	Cube (0.05)
Breakfast (5)	●	00035-00000006.soc	15	42	0.52	0.32	0.16	5-Cube (0.03)
Breakfast (6)	●	00035-00000007.soc	15	42	0.51	0.4	0.09	5-Cube (0.05)
Cycling (1)	▲	00043-00000002.soi	27	12	0.39	0.53	0.12	Mallows, norm- $\phi = 0.41$ (0.11)
Cycling (2)	▲	00043-00000010.soi	24	10	0.35	0.56	0.11	Mallows, norm- $\phi = 0.41$ (0.1)
Cycling (3)	▲	00043-00000025.soi	54	19	0.27	0.69	0.08	Mallows, norm- $\phi = 0.28$ (0.07)
Cycling (4)	▲	00043-00000026.soi	56	19	0.3	0.69	0.06	Mallows, norm- $\phi = 0.31$ (0.04)
Cycling (5)	▲	00043-00000033.soi	74	21	0.28	0.74	0.08	Mallows, norm- $\phi = 0.28$ (0.07)

Election Name	Marker	Preflib File	#Candidates	#Votes	Diversity	Agreement	Polarization	Closest Culture
Cycling (6)	▲	00043-00000071.soi	85	21	0.22	0.76	0.09	Single Peaked, Walsh (0.06)
Cycling (7)	▲	00043-00000085.soi	296	19	0.31	0.51	0.27	Urn, $\alpha = 0.29$ (0.08)
Cycling (8)	▲	00043-00000115.soi	178	22	0.22	0.65	0.12	Urn, $\alpha = 0.38$ (0.09)
Cycling (9)	▲	00043-00000117.soi	71	24	0.29	0.64	0.07	Mallows, $\text{norm-}\phi = 0.33$ (0.07)
Cycling (10)	▲	00043-00000187.soi	248	20	0.37	0.5	0.19	Urn, $\alpha = 0.37$ (0.12)
Universities (1)	◆	00046-00000001.soi	535	18	0.23	0.54	0.17	Urn, $\alpha = 0.29$ (0.06)
Universities (2)	◆	00046-00000002.soi	440	18	0.22	0.6	0.15	Urn, $\alpha = 0.38$ (0.07)
Universities (3)	◆	00046-00000003.soi	1180	19	0.22	0.57	0.24	Urn, $\alpha = 0.26$ (0.06)
Universities (4)	◆	00046-00000004.soi	1173	19	0.22	0.58	0.23	Urn, $\alpha = 0.26$ (0.07)
Spotify (1)	●	00047-00000021.soi	2242	54	0.09	0.9	0.02	Mallows, $\text{norm-}\phi = 0.1$ (0.02)
Spotify (2)	●	00047-00000033.soi	2294	54	0.09	0.9	0.02	Mallows, $\text{norm-}\phi = 0.1$ (0.02)
Spotify (3)	●	00047-00000098.soi	2192	54	0.09	0.89	0.02	Mallows, $\text{norm-}\phi = 0.1$ (0.02)
Spotify (4)	●	00047-00000099.soi	2146	54	0.09	0.89	0.02	Mallows, $\text{norm-}\phi = 0.1$ (0.02)
Spotify (5)	●	00047-00000119.soi	2292	54	0.09	0.9	0.02	Mallows, $\text{norm-}\phi = 0.1$ (0.02)
Spotify (6)	●	00047-00000146.soi	2277	54	0.09	0.9	0.03	Mallows, $\text{norm-}\phi = 0.1$ (0.02)
Spotify (7)	●	00047-00000164.soi	2413	54	0.09	0.9	0.02	Mallows, $\text{norm-}\phi = 0.1$ (0.02)
Spotify (8)	●	00047-00000283.soi	2633	53	0.08	0.9	0.02	Mallows, $\text{norm-}\phi = 0.1$ (0.02)
Spotify (9)	●	00047-00000307.soi	2609	51	0.09	0.9	0.02	Mallows, $\text{norm-}\phi = 0.1$ (0.02)
Spotify (10)	●	00047-00000362.soi	2681	53	0.09	0.89	0.02	Mallows, $\text{norm-}\phi = 0.1$ (0.02)
Movehub	◆	00050-00000001.soc	216	12	0.47	0.21	0.4	Urn, $\alpha = 0.31$ (0.11)
Countries (1)	◆	00051-00000002.soi	89	17	0.57	0.32	0.11	5-Cube (0.03)
Countries (2)	◆	00051-00000003.soi	102	17	0.57	0.31	0.1	5-Cube (0.04)
Countries (3)	◆	00051-00000004.soi	110	17	0.53	0.36	0.11	5-Cube (0.02)
Countries (4)	◆	00051-00000005.soi	114	19	0.61	0.29	0.1	10-Cube (0.02)
Countries (5)	◆	00051-00000006.soi	124	19	0.59	0.32	0.1	10-Cube (0.03)
Countries (6)	◆	00051-00000007.soi	146	19	0.6	0.3	0.12	5-Cube (0.03)
Countries (7)	◆	00051-00000008.soi	142	19	0.58	0.31	0.13	5-Cube (0.02)
Countries (8)	◆	00051-00000009.soi	137	18	0.59	0.29	0.12	5-Cube (0.02)
Countries (9)	◆	00051-00000010.soi	145	17	0.58	0.31	0.13	5-Cube (0.02)
Countries (10)	◆	00051-00000012.soi	141	15	0.55	0.29	0.19	5-Cube (0.05)
F1 (1)	▲	00052-00000002.soi	84	8	0.2	0.68	0.12	Single Peaked, Walsh (0.09)
F1 (2)	▲	00052-00000009.soi	87	11	0.19	0.72	0.08	Single Peaked, Walsh (0.04)
F1 (3)	▲	00052-00000018.soi	45	11	0.25	0.71	0.06	Mallows, $\text{norm-}\phi = 0.28$ (0.05)
F1 (4)	▲	00052-00000023.soi	42	12	0.36	0.6	0.09	Mallows, $\text{norm-}\phi = 0.4$ (0.07)
F1 (5)	▲	00052-00000035.soi	35	16	0.45	0.51	0.09	Mallows, $\text{norm-}\phi = 0.49$ (0.06)
F1 (6)	▲	00052-00000040.soi	47	16	0.35	0.61	0.08	Mallows, $\text{norm-}\phi = 0.36$ (0.07)
F1 (7)	▲	00052-00000042.soi	41	16	0.38	0.59	0.06	Mallows, $\text{norm-}\phi = 0.4$ (0.4)
F1 (8)	▲	00052-00000060.soi	25	17	0.38	0.56	0.11	Mallows, $\text{norm-}\phi = 0.41$ (0.09)
F1 (9)	▲	00052-00000067.soi	24	21	0.37	0.61	0.04	Mallows, $\text{norm-}\phi = 0.39$ (0.02)
F1 (10)	▲	00052-00000068.soi	25	20	0.31	0.65	0.06	Mallows, $\text{norm-}\phi = 0.33$ (0.05)
NSW (1)	■	00058-00000015.soi	5	47636	0.31	0.44	0.21	Urn, $\alpha = 0.49$ (0.01)
NSW (2)	■	00058-00000037.soi	6	49846	0.27	0.55	0.17	Urn, $\alpha = 0.29$ (0.05)
NSW (3)	■	00058-00000079.soi	8	48215	0.22	0.62	0.13	Urn, $\alpha = 0.38$ (0.07)
NSW (4)	■	00058-00000107.soi	7	45526	0.27	0.56	0.15	Urn, $\alpha = 0.29$ (0.08)
NSW (5)	■	00058-00000129.soi	6	48244	0.25	0.53	0.24	Urn, $\alpha = 0.29$ (0.03)
NSW (6)	■	00058-00000139.soi	6	47035	0.24	0.59	0.17	Urn, $\alpha = 0.38$ (0.08)
NSW (7)	■	00058-00000148.soi	4	51375	0.21	0.49	0.33	Urn, $\alpha = 0.66$ (0.03)
NSW (8)	■	00058-00000150.soi	6	50315	0.29	0.49	0.2	Urn, $\alpha = 0.29$ (0.05)
NSW (9)	■	00058-00000183.soi	8	47857	0.24*	0.63	0.11*	Urn, $\alpha = 0.38$ (0.1)
NSW (10)	■	00058-00000235.soi	7	51633	0.3	0.54	0.13	Urn, $\alpha = 0.29$ (0.1)

Table 3: The elections from Preflib included in the maps in Figures 4 and 10 along with the values of their Diversity, Agreement, and Polarization indices. The values denoted with \* has been computed as the average value for 20 elections with 500 votes sampled from the given election. In the last column we provide the closest artificial election to a given Preflib election in terms of DAP distance and the distance itself (in the parenthesis).